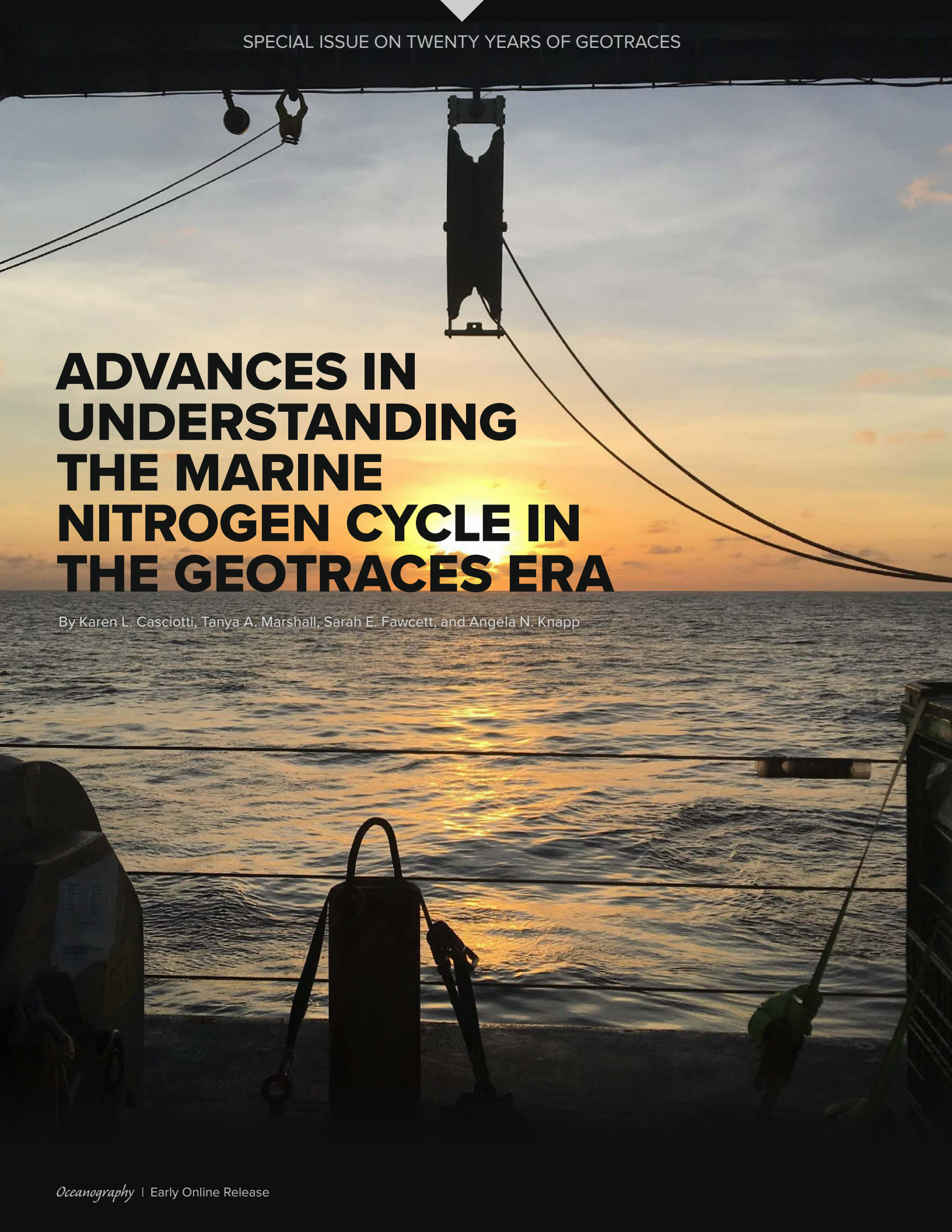

ADVANCES IN UNDERSTANDING THE MARINE NITROGEN CYCLE IN THE GEOTRACES ERA

By Karen L. Casciotti, Tanya A. Marshall, Sarah E. Fawcett, and Angela N. Knapp

ABSTRACT. Because nitrogen availability limits primary production over much of the global ocean, understanding the controls on the marine nitrogen inventory and supply to the surface ocean is essential for understanding biological productivity and exchange of greenhouse gases with the atmosphere. Quantifying the ocean's inputs, outputs, and internal cycling of nitrogen requires a variety of tools and approaches, including measurements of the nitrogen isotope ratio in organic and inorganic nitrogen species. The marine nitrogen cycle, which shapes nitrogen availability and speciation in the ocean, is linked to the elemental cycles of carbon, phosphorus, and trace elements. For example, the majority of nitrogen cycle oxidation and reduction reactions are mediated by enzymes that require trace metals for catalysis. Recent observations made through global-scale programs such as GEOTRACES have greatly expanded our knowledge of the marine nitrogen cycle. Though much work remains to be done, here we outline key advances in understanding the marine nitrogen cycle that have been achieved through these analyses, such as the distributions and rates of dinitrogen fixation, terrestrial nitrogen inputs, and nitrogen loss processes.

INTRODUCTION

Globally, biological dinitrogen (N_2) fixation provides the majority of bioavailable nitrogen (N) to the ocean, with additional contributions from atmospheric deposition, river runoff, and submarine groundwater discharge (SGD; Figure 1). These processes contribute to the inventory of bioavailable N in the forms of nitrate (NO_3^-), nitrite (NO_2^-), and ammonium (NH_4^+), as well as particulate and dissolved organic N (PON and DON, respectively), all of which are considered "fixed" N.

Bioavailable N is cycled among these forms through assimilation processes whereby inorganic and dissolved organic forms of N are incorporated into biomass (PON), and the reverse, whereby PON is degraded to DON and ammonium (Figure 1). Reduced N in the forms of ammonium and DON can then be oxidized to nitrite and nitrate through nitrification, which produces nitrous oxide (N_2O) as a byproduct (Stein, 2019; Wan et al., 2023). Alternatively, uptake of these reduced forms of N by primary producers supports regenerated production, which is defined as phytoplankton growth using N sourced from within the sunlit (euphotic) zone (Dugdale and Goering, 1967). By contrast, new and export production are fueled by N supplied to the euphotic zone via N_2 fixation, atmospheric deposition, fluvial inputs, laterally transported organic nutrients, and/or upward transport of nitrate from the aphotic zone (Dugdale and Goering, 1967; Eppley and Peterson, 1979; Figure 1).

Nitrogen loss occurs through N_2 production via the processes of denitrification and anaerobic ammonia oxidation (anammox) in anoxic sediments and water parcels (Figure 1). Because N_2 is not widely bioavailable, its production is considered a loss of bioavailable N from the marine environment. The burial of organic N that escapes degradation in the water column and shallow sediments is the other main loss of bioavailable N from the water column. Of these, benthic denitrification is perhaps the largest sink for bioavailable N, although estimates of N loss range widely and are a key uncertainty in the marine N budget (Gruber and Sarmiento, 1997; Brandes and Devol, 2002; Codispoti, 2007; DeVries et al., 2013; Wang et al., 2019).

The N cycle is unique among marine elemental cycles in being primarily driven by biological processes. As described above, the main inputs and losses of bioavailable N, as well as its internal cycling, rely on the activities of specialized microbial metabolisms. The enzymes that catalyze N oxidation and reduction reactions can be some of the most abundant proteins in the global ocean (Saito et al., 2020), and because they rely on metal cofactors at their active sites (Morel and Price, 2003), their activity can be limited by trace metal availability (Morel et al., 2020). A classic example is the limitation of nitrate assimilation in high-nutrient, low-chlorophyll regions by low iron availability (Martin et al., 1991). Iron is also required for enzymes involved in N_2 fixation, as well as some steps of nitrification (Wei et al., 2006; Ferguson et al., 2007; Shafiee et al., 2019), denitrification (Zumft, 1997), and anammox (Kartal and Keltjens, 2016) (Figure 1). Thus, the

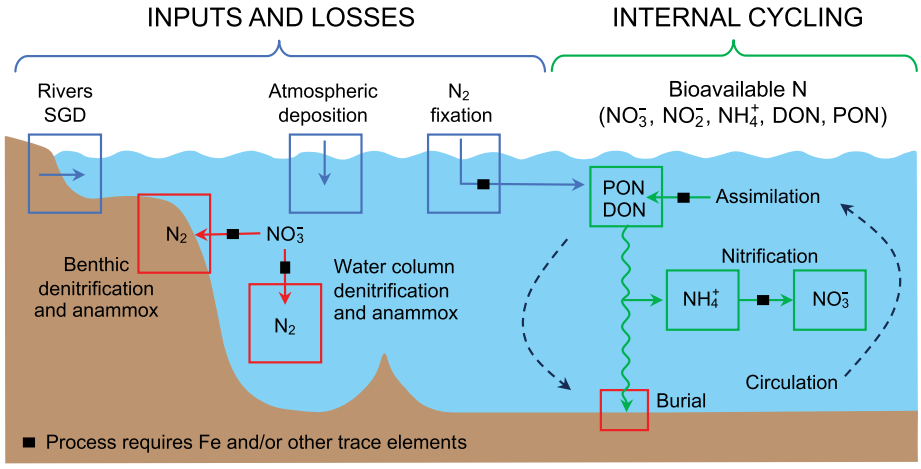

FIGURE 1. Schematic of the marine nitrogen cycle showing the major fixed N inputs (blue arrows) of rivers, submarine groundwater discharge (SGD), atmospheric deposition, and N_2 fixation; losses (red arrows) via benthic and water column denitrification and anammox and organic N burial; and internal cycling processes (green arrows) of assimilation, ammonification, and nitrification. Processes requiring iron (Fe) and/or other trace metal cofactors are indicated with black squares overlaid on the arrows. Ocean circulation is represented with dashed arrows. *Figure modified with permission from Fitzsimmons and Conway (2023)*

utilization of nitrogenous substrates for assimilation or energy generation can be affected not only by the availability of those substrates but also by the availability of trace metals for enzyme activity (Morel et al., 2020; Rafter, 2024, in this issue). Understanding the distribution of processes involved in the marine N cycle and budget is thus aided by considering trace metal availability in the environment.

Nutrient Stoichiometry

Accurate estimates of N inputs and losses are necessary for a first-order constraint on the oceanic N inventory, which has implications for better understanding ocean fertility and climate. The quantities of fixed N supply to and loss from the ocean have been widely explored through the distributions of nitrate and phosphate (PO_4^{3-}) concentrations, which are routinely measured on oceanographic expeditions. Combining these nutrient measurements to compute the tracer N*, typically defined as $[NO_3^-] - 16 \times [PO_4^{3-}]$, has been instrumental in mapping and quantifying N_2 fixation and N loss in the Atlantic and Pacific Oceans (Gruber and Sarmiento, 1997; Deutsch et al., 2001). Subsequently, surface distributions of P*, typically defined as $[PO_4^{3-}] - [NO_3^-] \div 16$ (Deutsch et al., 2007), have been used to diagnose regions that may favor N_2 fixation, where positive P* values indicate the availability of PO_4^{3-} in excess of stoichiometric N requirements (Deutsch et al., 2007; Moore et al., 2009). The surface layer convergence of P* computed by ocean circulation models has also been used to quantify N_2 fixation, by attributing the consumption of excess PO_4^{3-} to N_2 fixation (Deutsch et al., 2007; Wang et al. 2019). These estimates provide some of the most spatially integrated evaluations of basin-scale N input and loss but are sensitive to locally significant atmospheric and riverine inputs, as well as internal cycling through variations in the N:P ratio of nutrients incorporated into and released from organic matter (Arrigo, 2005; Mills and Arrigo, 2010; Martiny et al., 2013; Wang et al., 2019; Liang et al., 2023). Further, in regions where N_2 fixation and denitrification may both impact nutrient ratios, those signals counteract each other, leading to a net effect that diminishes the signal of both N input and N loss in inorganic nutrient distributions (Sigman et al., 2005; Yoshikawa et al., 2015). These limitations can be overcome by complementary measurements of biogenic N_2 distributions (Chang et al., 2010; DeVries et al., 2012), instantaneous production rates (Moore et al., 2009; Yoshikawa et al., 2015; Shao et al., 2023), and stable isotope ratios (see below).

Isotopic Systematics

The N and oxygen (O) isotope ratios in nitrate ($^{15}R_{NO3}$ and $^{18}R_{NO3}$, respectively) provide an alternate view of nitrate input, loss, and internal cycling in the ocean. The mean ocean nitrate $\delta^{15}N$,

$$\delta^{15}N\ (‰) = (^{15}R_{NO3}/^{15}R_{N2} - 1) \times 1{,}000,$$

where $^{15}R_{N2}$ is the N isotope ratio of N_2 in air, is around 5‰ (Sigman et al., 2000), set by the balance between the input of N with a low $\delta^{15}N$ from N_2 fixation and the isotopic fractionation imposed by N loss via denitrification (and anammox) in the water column and marine sediments (Brandes and Devol, 2002). Water column denitrification, in particular, causes a large increase in nitrate $\delta^{15}N$ for a given amount of nitrate consumed, whereas benthic denitrification causes relatively little change in nitrate $\delta^{15}N$ (Cline and Kaplan, 1975; Brandes et al., 1998). There has also been recent recognition of a role for isotopic fractionation during nitrate consumption in the Southern Ocean in modulating mean ocean nitrate $\delta^{15}N$ (Fripiat et al., 2023). The mean nitrate $\delta^{18}O$,

$$\delta^{18}O\ (‰) = (^{18}R_{NO3}/^{18}R_{VSMOW} - 1) \times 1{,}000,$$

where $^{18}R_{VSMOW}$ is the O isotope ratio in Vienna Standard Mean Ocean Water (VSMOW), is approximately 2‰ (Casciotti et al., 2002; Sigman et al., 2005). In contrast to mean ocean nitrate $\delta^{15}N$, this mean $\delta^{18}O$ value is predominantly controlled by nitrification, which adds O atoms to the nitrate pool, and nitrate assimilation, which removes them (i.e., internal N cycle processes; Sigman et al., 2005; Rafter et al., 2013). Water column denitrification plays a lesser role in setting the average deep ocean nitrate $\delta^{18}O$ because it represents a smaller global flux than nitrate assimilation, which is the dominant sink for nitrate O isotopes. Measurements of nitrate $\delta^{15}N$ and $\delta^{18}O$ thus allow overlapping N cycle processes to be disentangled, often through their difference as the tracer $\Delta(15–18) = \delta^{15}N - \delta^{18}O$ (Sigman et al., 2005; Rafter et al., 2013).

For example, during nitrate assimilation and denitrification, the O isotopes in nitrate are fractionated to approximately the same extent as the N isotopes, so that the $\delta^{18}O$ and $\delta^{15}N$ of the nitrate pool rise in a ratio of 1:1 as consumption proceeds (Casciotti et al., 2002; Granger et al., 2004, 2008, 2010; Karsh et al., 2012; Rohde et al., 2015). As a result, these processes lead to no change in nitrate $\Delta(15–18)$ (Rafter et al., 2013). In contrast, the remineralization (via ammonification and nitrification) of PON yields nitrate with a $\delta^{15}N$ that roughly equals that of the PON being regenerated while its $\delta^{18}O$ is set by nitrification, which incorporates the $\delta^{18}O$ of seawater (typically ~0‰) plus an isotopic offset of ~1.1‰ (Sigman et al., 2009; Buchwald et al., 2012; Marconi et al., 2015, 2019; Boshers et al., 2019). When nitrification occurs coincident with partial nitrate assimilation, the $\delta^{18}O$ of the combined (i.e., partially assimilated plus newly nitrified) nitrate pool initially increases while its $\delta^{15}N$ is unaltered, leading to a decline in $\Delta(15–18)$ (Wankel et al., 2007; Sigman et al., 2009; Rafter et al., 2013; Fawcett et al., 2015). While the remineralization of newly fixed N can also cause nitrate $\Delta(15–18)$ to decline, this change is due to a stronger decrease in nitrate $\delta^{15}N$ than $\delta^{18}O$ (Knapp et al., 2008; Rafter et al., 2013; Marshall et al., 2023). As such, the influence of N_2 fixation on nitrate isotopes can be separated from that of coupled partial nitrate assimilation and nitrification (Fawcett et al., 2015; Marshall et al., 2023). By

investigating the regional- and basin-scale distributions of nitrate $\delta^{15}N$ and $\delta^{18}O$ (Figure 2), we aim to understand the balance of processes affecting the N inventory. More background on nitrate isotope applications in the ocean is available in the original literature and recent overviews (Casciotti, 2016b; Sigman and Fripiat, 2019). Here, we aim to illustrate how major questions in marine N cycle research have been informed by basin-scale measurements of nitrate isotopes, such as: what are the rates and controls on the N inputs and losses that govern the marine N budget on a global scale, and what are the dominant forms of and supply routes for N fueling biological production and altering the health of ecosystems? We additionally consider insights gleaned from measurements of dissolved organic nutrients and the $\delta^{15}N$ of DON.

NITROGEN INPUTS TO THE OCEAN

Biological N_2 Fixation

Geochemical tracers such N* and nitrate $\delta^{15}N$ provide a spatially integrative approach to identifying and quantifying N input through N_2 fixation. The $\delta^{15}N$ of *Trichodesmium*, a widespread tropical diazotroph, ranges from –2‰ to 0‰ (Carpenter et al., 1997; Karl et al., 1997; Montoya et al., 2002; Holl et al., 2007), which is significantly lower than thermocline and deep ocean nitrate $\delta^{15}N$ (2‰–7‰; Figure 3; Sigman et al., 2000; Knapp et al., 2008; Rafter et al., 2013, 2019; Fripiat et al., 2021a). The remineralization of newly fixed organic matter thus lowers nitrate $\delta^{15}N$ while raising N* by introducing nutrients with a high N:P ratio (i.e., 25:1 to 50:1; White et al., 2006; Knapp et al., 2012) relative to mean ocean N:P (i.e., ~16:1; Redfield et al., 1963).

N_2 fixation rates can be estimated by coupling these geochemical tracer distributions with information on ocean circulation. Inferred estimates of N_2 fixation that rely on N* necessarily involve assumptions of the N:P stoichiometry of N_2 fixing (diazotrophic) and non-diazotrophic plankton. These estimates suggest that N_2 fixation predominantly occurs in the warm, well-lit low latitude ocean but with zonal differences (Gruber and Sarmiento, 1997; Deutsch et al., 2007; Moore et al., 2009; Wang et al., 2019). At a global scale, higher N_2 fixation rates in the Pacific (95–100 Tg N yr^{-1}) than in the Atlantic (20–34 Tg N yr^{-1}) and the Indian Oceans (22–27 Tg N yr^{-1}) suggest that while N gain is greatest in the Pacific, this ocean basin is actually a net sink for N (Luo et al., 2012; Landolfi et al., 2018; Wang et al., 2019). However, gaps in global ocean nutrient distributions (e.g., the South Atlantic and much of the Indian Ocean) as well as observed temporal and spatial variability in organic matter N:P ratios (White et al., 2006; Martiny et al., 2013; Liang et al., 2023) leave open the possibility for new insights into the rates and distribution of N_2 fixation, particularly in the Southern Hemisphere.

The addition of isotopic measurements to basin-wide transects has provided new insights into the distribution of N_2 fixation in the global ocean. For example, some of the first efforts to combine nitrate $\delta^{15}N$ data from a transect in the western subtropical North Atlantic with an ocean model yielded a whole Atlantic N_2 fixation rate of 15–24 Tg N yr^{-1} (Knapp et al., 2008). This N isotope-based estimate is remarkably consistent with one based on N* and volume fluxes from transects across the Atlantic, of 15–21 Tg N yr^{-1} (Moore et al., 2009). Notably, these geochemical signals ($\delta^{15}N$ and N*) manifest most strongly in the thermocline,

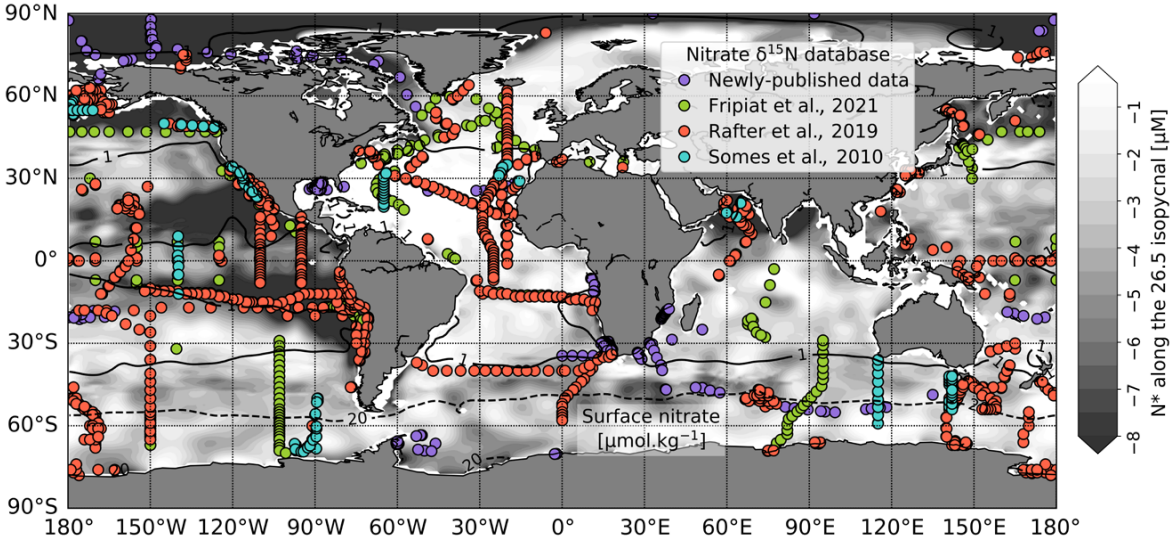

FIGURE 2. Map of the published global ocean nitrate $\delta^{15}N$ databases from 2010 to 2024. The background color indicates N* (= $[NO_3^-] - 16 \times [PO_4^{3-}]$) in µM along the 26.5 kg.m^{-3} isopycnal, which is where some of the lowest N* signals occur in the Pacific and some of the highest in the Atlantic. The solid and dashed black contours indicate the 1 and 20 µM surface nitrate concentrations, respectively. N* and nitrate concentration data are from the World Ocean Atlas 2018 (Garcia et al., 2018). Symbol color indicates the database in which observations were first included (see legend). Supplementary Table S1 provides references for new data included in the 2024 update.

where remineralized products accumulate (Figure 2), and integrate over the spatial and temporal scales of that water mass, so they do not necessarily represent in situ rates. For example, the low-$\delta^{15}N$ nitrate observed in the Sargasso Sea thermocline is largely representative of a basin-wide N_2 fixation signal rather than incidences of local N_2 fixation (Knapp et al., 2008; Marconi et al., 2015).

In addition, the thermocline nitrate concentration affects the $\delta^{15}N$ signal. In the North Atlantic along the cross-basin GEOTRACES GA03 transect (35°N, 70°W to 18°N, 15°W), a strong positive correlation was observed between the concentration and $\delta^{15}N$ of thermocline nitrate, with both parameters decreasing from east to west (Figure 3; Marconi et al., 2015). The authors concluded that the low nitrate concentration at the top of the thermocline acts to focus the low $\delta^{15}N$ signal deriving from the regeneration of newly fixed N, such that the observed zonal decrease in thermocline nitrate $\delta^{15}N$ does not require a coincident increase in the N_2 fixation rate. Quantification of the meridional flux of nitrate $\delta^{15}N$ and N* across multiple zonal transects of the Atlantic Ocean has also revealed that N_2 fixation predominantly occurs in the tropical Atlantic between 11°S and 24°N (Marconi et al., 2017b).

In the subtropical South Pacific (~17°S) and South Indian (~32°S) Oceans, zonal transects of nitrate $\delta^{15}N$ and/or N* suggest that N_2 fixation occurs largely in the western subtropics and is negligible to the east (Grand et al., 2015; Yoshikawa et al., 2015), consistent with regional studies from the boundaries of both basins (Knapp et al., 2016a, 2018; Bonnet et al., 2017, 2023; N. Lehmann et al., 2018; Forrer et al., 2023; Marshall et al., 2023). N_2 fixation also appears to be limited in the central subtropical South Atlantic (Moore et al., 2009) and South Pacific (Peters et al., 2018b) where iron availability (Figure 3b) and the aeolian iron supply to surface waters are low (Jickells et al., 2005; Mahowald et al., 2009). This notion is borne out by existing nitrate isotope sections that do not show a pervasive signal of low $\delta^{15}N$ nitrate in the subtropical South Atlantic thermocline between 35° and 40°S (Figure 3a; Tuerena et al., 2015; Marconi et al., 2017b). However, across the tropical South Atlantic (~12°S), signals of N_2 fixation are apparent in the Angola Gyre in the east, yet not in the west (Marshall et al., 2022) (Figure 4a). These zonally heterogeneous distributions of N_2 fixation across the low latitudes suggest that N_2 fixation may not occur as homogeneously as some models predict, and more importantly, that the controls on N_2 fixation are dependent on regional P and iron availability, as discussed below.

Converging Controls on N_2 Fixation

Diazotrophs can be limited by both iron and P (Berman-Frank et al., 2001; Mills et al., 2004; Held et al., 2020). Large-scale sampling of N_2 fixation proxies (e.g., nitrate $\delta^{15}N$, N*, ^{15}N incubation

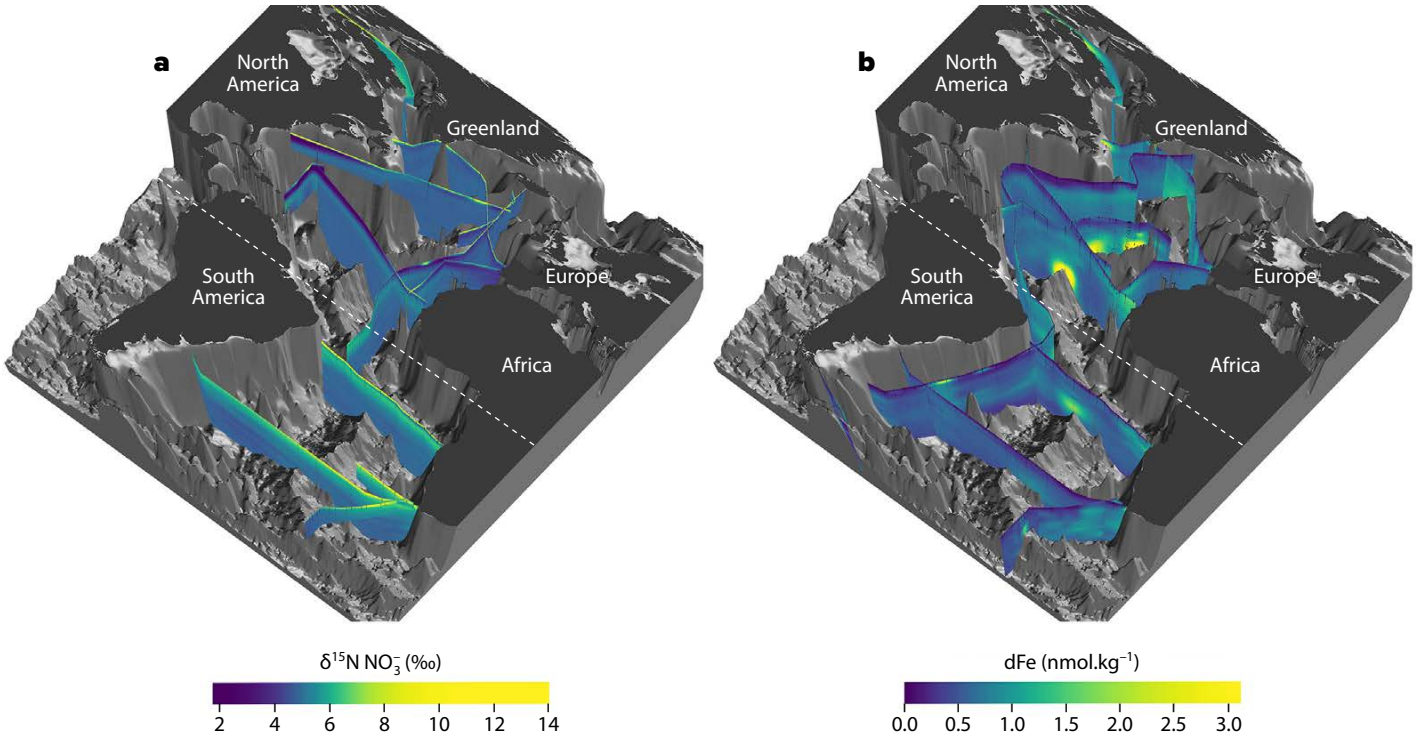

FIGURE 3. Three-dimensional visualization of (a) nitrate $\delta^{15}N$ (‰ vs. air), and (b) dissolved iron (dFe; nmol.kg^{-1}) in the Atlantic Ocean. In each panel, low values are shown in blue and high values are shown in yellow. Nitrate $\delta^{15}N$ data in panel a were obtained from the locations shown in Figure 2 (Somes et al., 2010; Rafter et al., 2019; Fripiat et al., 2021b), and the dissolved iron data from the same region (panel b) are from GEOTRACES IDP2021v2 (GEOTRACES Intermediate Data Product Group, 2023). The dashed white line indicates the equator. *3D graphics created by Reiner Schlitzer, Alfred Wegener Institute*

experiments, diazotroph abundances) coincident with measurements of dissolved iron and (in)organic P pools suggest that N_2 fixation is driven by both the availability of iron and excess P. In other words, where iron is locally available, excess P is taken up by diazotrophs to fix N_2 (Deutsch et al., 2007; Moore et al., 2009; Weber and Deutsch, 2014; Snow et al., 2015; Wang et al., 2019). For example, in the North Atlantic where iron is often non-limiting (Figure 3b), diazotrophs appear to use excess P (including both PO_4^{3-} and dissolved organic P, DOP) to fix N_2 (Dyhrman and Ruttenberg, 2006; Sohm and Capone, 2006; Orchard et al., 2010; Landolfi et al., 2015), while in the South Atlantic where excess PO_4^{3-} is present, diazotrophs appear to use non-aeolian iron to fix N_2 (Marshall et al., 2022; Figure 4b). In the subtropical North Pacific Ocean, elevated N_2 fixation rates have recently been surmised to be jointly regulated by iron and P availability (Wen et al., 2022; Horii et al., 2023). Similarly, in the Southwest Indian Ocean, elevated N_2 fixation rates coincide with an overlapping supply of aeolian and sedimentary iron and excess P (Grand et al., 2015; Chowdhury et al., 2023; Marshall et al., 2023).

Improvement in our understanding of the sources, distributions, and cycling of both iron and P over the last decade has contributed to the discovery of new regions of N_2 fixation (Zehr and Capone, 2020). For many years, dust deposition was considered the only quantitatively important source of iron to the ocean, with other iron sources thought to contribute negligibly to the euphotic zone (Mahowald et al., 2005). More recently, however, non-aeolian iron sources (e.g., oxygenated and anoxic ocean sediments, hydrothermal vents, and sea ice) are increasingly being recognized as quantitatively important (Tagliabue et al., 2010, 2022; Conway and John, 2014; Rijkenberg et al., 2014; Resing et al., 2015; Fitzsimmons et al., 2017; Jenkins et al., 2020; Homoky et al., 2021; Fitzsimmons and Conway, 2023), including for alleviating regional diazotroph iron limitation (Bonnet et al., 2023). In concert, our understanding of P cycling, and its utilization by diazotrophs, has improved, aided by an expanding DOP database (Liang et al., 2022b).

The three major oxygen deficient zones (ODZs; i.e., the eastern tropical North and South Pacific [ETNP and ETSP, respectively], and the Arabian Sea) have presented specific challenges to our understanding of the controls on N_2 fixation using the geochemical tracers discussed above, due to the opposing effects of N_2 fixation and denitrification on N* and nitrate $\delta^{15}N$. In these areas, the upwelling and offshore advection of iron- and P-replete (N-deplete) waters from the ODZ appear to generate ideal conditions for N_2 fixation (Deutsch et al., 2007); however, the observations are inconsistent as to the importance of N_2 fixation in these regions, with some studies indicating considerable N_2 fixation (Capone et al., 1998; Sigman et al., 2005; Fernandez et al., 2011) and others indicating that N_2 fixation rates can be exceedingly low (Turk-Kubo et al., 2014; Berelson et al., 2015; Knapp et al., 2016a). The spatial decoupling of excess P and iron availability could explain the inconsistency, with iron being more quickly depleted in nearshore waters than P, thus limiting N_2 fixation despite the presence of excess P (Fernandez et al., 2011; Dekaezemacker et al., 2013; Jayakumar et al., 2017). Another explanation relates to the variable time and depth scales over which iron, P, nitrate $\delta^{15}N$, N*, and N_2 fixation experiments integrate. For example, $^{15}N_2$ fixation rates are often measured over a day or less (Montoya et al., 1996; Luo et al., 2012; White et al., 2020; Shao et al., 2023), while iron recycling can occur over days to weeks (Boyd and Ellwood, 2010; Rafter et al., 2017; Tagliabue et al., 2019) and the accumulation of newly fixed N as nitrate in the thermocline integrates over years to decades (Gruber and Sarmiento, 1997). The variability associated with P and iron limitation on N_2 fixation over various spatial (i.e., intra- and inter-basin) and temporal scales suggests that iron exerts the dominant control on regional N_2 fixation rates and that P in excess of N exerts the dominant control on global N_2 fixation rates (Weber and Deutsch, 2014; Wen et al., 2022).

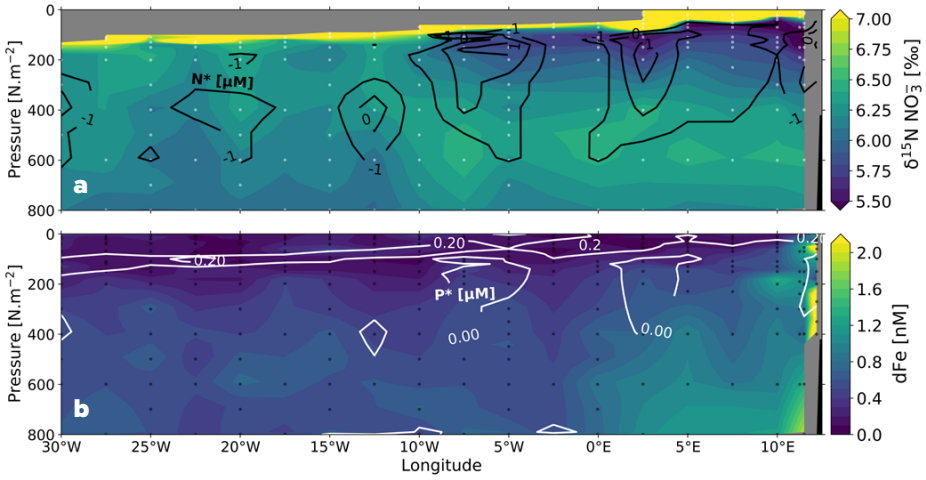

FIGURE 4. Zonal depth sections across the tropical South Atlantic Ocean (CoFeMUG along ~11°S) of (a) nitrate $\delta^{15}N$ (‰ vs. air) with black contours indicating N* (= $[NO_3^-]$ – 16 × $[PO_4^{3-}]$) (µM), and (b) dissolved iron (dFe, nM) with white contours indicating P* (= $[PO_4^{3-}]$ – $[NO_3^-]$ ÷ 16) (µM) (Noble et al., 2012; Marconi et al., 2017b; Marshall et al., 2022). On panel a, low-$\delta^{15}N$ nitrate and elevated N* in the Angola Gyre thermocline (east of 10°W, 50–400 m) both signal N_2 fixation, neither of which are apparent in the western portion of the CoFeMUG transect. On panel b, elevated dissolved iron concentrations supplied by the margin overlap with elevated surface P* in the Angola Gyre; the coincidence of these two conditions appears to favor N_2 fixation.

Atmospheric and Margin Influences on the Marine Nitrogen Cycle

Globally, atmospheric deposition contributes 39–90 Tg N yr^{-1} and river runoff contributes 11–43 Tg N yr^{-1} to the ocean (Duce et al., 1991; Seitzinger et al., 2010; Yang and Gruber, 2016; Jickells et al., 2017; Wang et al., 2019). Submarine groundwater discharge (SGD), while poorly constrained, likely adds fluxes of N comparable in magnitude to rivers (Santos et al., 2021). For a comprehensive review on N cycling between the atmosphere and surface ocean, including the use of geochemical tracers such as nitrate $\delta^{15}N$ and N*, see Altieri et al. (2021).

The riverine N flux is small relative to other N sources and is also highly regional, making it difficult to quantify. In addition, at least a quarter of river-derived N fails to reach the open ocean and is instead trapped by intense recycling over the shallow continental shelves (Jickells et al., 2017; Sharples et al., 2017; Izett and Fennel, 2018). For example, Mississippi River nitrate, which has a distinct $\delta^{15}N$ of 8‰ (Bryant-Mason et al., 2013), has not been detected in the off-shelf waters in the Gulf of Mexico (Howe et al., 2020; Knapp et al., 2022), most likely because it is consumed in nearshore waters (Rabalais et al., 1996). Nevertheless, the Amazon River has been found to enhance regional ocean productivity by supplying N, along with excess P and iron that fuel local N_2 fixation (Subramaniam et al., 2008). Similarly, the Congo River margin supplies a significant flux of iron to the eastern tropical South Atlantic (Noble et al., 2012; Vieira et al., 2020) that appears to support regional N_2 fixation (Sohm et al., 2011; Marshall et al., 2022).

The $\delta^{15}N$ of nitrate and DON from river runoff and SGD are perhaps the most unconstrained N sources to the ocean, with measurements of nitrate $\delta^{15}N$ from rivers ranging from –3‰ to 28‰ and averaging 7.1‰, and from shallow aquifers ranging from 2‰ to 27‰ and averaging 7.7‰ (Matiatos et al., 2021). Each of these sources may have distinct relationships with trace elements, but few studies include measurements of dissolved metal concentrations and nitrate isotopes, or DON and DOP concentrations and DON $\delta^{15}N$ to constrain source relationships, especially in margin environments where multiple sources may mix. Existing datasets from nearshore regions show significant correlations between concentrations of dissolved organic matter (DOM), salinity, and/or trace metal concentrations associated with rivers and/or continental shelves (Chen et al., 2022, 2023). For example, along the oligotrophic West Florida Shelf (WFS; Figure 5a), significant correlations of DON and dissolved iron concentrations have been observed (Figure 5b; Mellett and Buck, 2020). Here, high concentrations of DON and dissolved iron in nearshore waters give way in offshore waters to lower concentrations consistent with those observed in the oligotrophic North Atlantic, i.e., ~4–5 µM DON and <1 nM dissolved iron, respectively (Knapp et al., 2011; Hatta et al., 2015). The highly correlated concentration gradients on the WFS have been interpreted as indicating common margin sources of DON and trace metals, raising questions about how DON from margin sources such as SGD may serve as a ligand for trace metals and thus impact their transfer from nearshore to offshore environments (Beck et al., 2007, 2010).

Allochthonous Dissolved Organic Nutrient Fluxes

Decades of work have shown that about 20% of new production is released as DOC (Hansell and Carlson, 1998; Romera-Castillo et al., 2016), and recent work suggests similar relationships for DON (Letscher et al., 2013; Knapp et al., 2018; Zhang et al., 2020) and DOP (Liang et al., 2023). These findings are consistent with field-based incubation studies showing that DON is preferentially released by phytoplankton when grown on "new" sources of N, including nitrate (Bronk and Ward, 1999, 2000) and N_2 (Capone et al., 1994; Glibert and Bronk, 1994; Bonnet et al., 2016; Knapp et al., 2016b). Observations suggest that there is net DON and DOP production in coastal and other upwelling areas, with advection of DON and DOP into the oligotrophic gyres (Letscher et al., 2013; Liang et al., 2022a) where they may be used to support a significant fraction of new and export production (Letscher et al., 2013, 2022; Knapp et al., 2018; Liang et al., 2022a, 2023).

Many of the enzymes that enable dissolved organic nutrient assimilation have metal co-factors. These include urease, which requires nickel (Dupont et al., 2008); enzymes allowing the use of primary amines and/or amino acids, which require copper (Palenik and Morel, 1991); and enzymes supporting the utilization of various forms of DOP, which require zinc, cadmium, cobalt, and/or iron (Duhamel

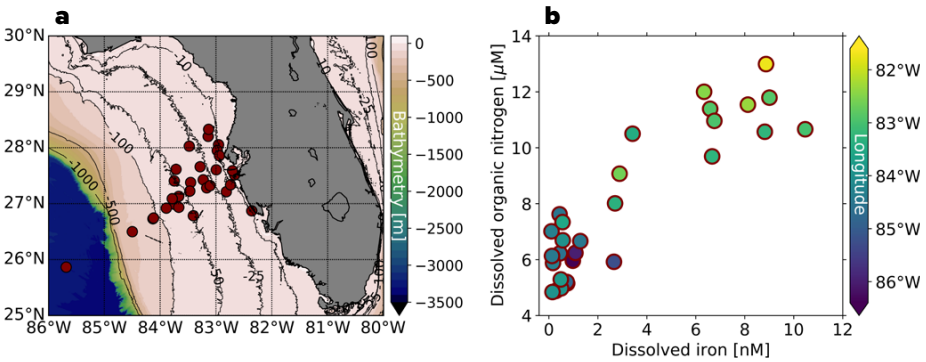

FIGURE 5. (a) Map of West Florida Shelf stations sampled in June 2015 and February-March 2018, and (b) dissolved organic nitrogen (DON, µM) versus dissolved iron concentrations (dFe, nM) at these stations, with symbol color indicating station longitude. DON is highly correlated with dissolved iron (r^2 =0.89 for 2015 and r^2 =0.91 for 2018). The dissolved iron data were previously published in Mellett and Buck (2020). DON was measured according to Knapp et al. (2005).

et al., 2021). Thus, it would perhaps be unsurprising if DON and DOP distributions correlated with dissolved metal availability in the surface ocean. However, few studies of marine DOM cycling have also included measurements of dissolved trace metal concentrations, limiting our understanding of the extent to which DOM release by new production is influenced by trace metal availability. Because dissolved organic nutrients fuel a significant fraction of export production in oligotrophic gyres, our poor understanding of the controls on marine DOM production means we lack constraints on an important source of nutrients.

Additionally, while dissolved organic nutrient fluxes from ocean margins to gyres are required by models to resolve oligotrophic nutrient budgets (Torres-Valdes et al., 2009; Letscher et al., 2016, 2022), surface ocean concentration gradients have been challenging to document due to the sparse datasets for DOP, and for DON, by the poor precision of high temperature chemical oxidation measurements of its concentration (Letscher et al., 2013). New DON (Hansell et al., 2021) and DOP (Liang et al., 2022b) concentration datasets should improve our understanding of spatial distributions. Additionally, new measurements of DON concentration using higher-sensitivity wet-chemical oxidation methods paired with the analysis of DON $\delta^{15}N$ have revealed patterns of both DON production and consumption. For example, DON consumption was inferred from its isotopic variations for the first time in the eastern tropical South Pacific (Knapp et al., 2018) and was later confirmed in the South China Sea (Zhang et al., 2020). Cross-basin sections pairing DON concentration measured by wet-chemical oxidation methods, DON $\delta^{15}N$ analyses, and trace metal concentration and speciation measurements are now being made for some GEOTRACES and GO-SHIP transects, providing constraints on the role of trace metal availability in dissolved organic matter production and consumption.

INTERNAL CYCLING OF NITROGEN IN THE OCEAN

Nitrogen Speciation, Transport, and Uptake in the Euphotic Zone

The internal cycling of N in the ocean strongly affects the distribution of the N species and their isotopes. In this section, we focus on the imprint of the internal N cycle on the isotopes of nitrate, as this is the species predominantly measured as part of global-scale programs such as GEOTRACES. In addition, nitrate is the major subsurface source of fixed N for phytoplankton, and its residence time is longer than that of many other fixed N species such as ammonium, nitrite, and labile DON; thus, processes that alter the isotopic composition of nitrate exert a dominant control on the distribution of oceanic N isotopes. This is especially true in water masses sourced from the Southern Ocean (e.g., Antarctic Intermediate Water, AAIW; Subantarctic Mode Water, SAMW), which supply nitrate to the global thermocline (see below).

An early examination of nitrate N isotope data from samples collected along transects of the eastern Indian (WOCE I09S) and Pacific (ANT XII/4) sectors of the Southern Ocean (Sigman et al., 1999, 2000) revealed a strong negative correlation between nitrate concentration and $\delta^{15}N$ in the surface layer. This relationship is due to the preferential assimilation of ^{14}N-bearing nitrate by phytoplankton (i.e., isotope fractionation), which causes ^{15}N enrichment of the residual nitrate pool relative to the immediate source of nutrients to the surface layer (Sigman et al., 1999; Altabet, 2001; Karsh et al., 2003; Lourey et al., 2003). Investigations of large-scale sections of nitrate $\delta^{15}N$ and $\delta^{18}O$ have revealed that nitrate assimilation is typically the dominant biological process acting on the surface nitrate pool (cyan arrow in Figure 6a), with little room for sustained in situ nitrification (Rafter et al., 2013; Marconi et al., 2015; Tuerena et al., 2015; Fripiat et al., 2019; Marshall et al., 2023). A notable exception is the Antarctic Zone of the Southern Ocean, where winter conditions are extremely unfavorable for phytoplankton growth. Smart et al. (2015) measured the dual isotopes of nitrate along WOCE line A12 between 52.0°S and 57.8°S in austral winter and found the $\delta^{18}O$ of mixed-layer nitrate to be strongly elevated relative to its $\delta^{15}N$ (purple arrows in Figure 6b), characteristic of in situ nitrification, with the newly produced nitrate having a $\delta^{15}N$ of <–5‰ (i.e., set by the PON plus ammonium being remineralized) and a $\delta^{18}O$ of +1.1‰ (Sigman et al., 2005; Wankel et al., 2007). In the Antarctic Zone mixed layer, nitrate assimilation and nitrification appear to occur dominantly in summer and winter, respectively, with the apparent wintertime rise in nitrate $\delta^{15}N$ and $\delta^{18}O$ toward the surface due not to assimilation but to mixing between the summer/autumn mixed layer (lower nitrate concentration, higher $\delta^{15}N$ and $\delta^{18}O$) and underlying Circumpolar Deep Water (higher nitrate concentration, lower $\delta^{15}N$ and $\delta^{18}O$) (Smart et al., 2015).

Nitrate isotope sections are particularly powerful for investigating how N cycle processes occurring in geographically limited regions are connected via large-scale ocean circulation. Rafter et al. (2013) used measurements of nitrate $\delta^{15}N$ and $\delta^{18}O$ from the Pacific—CLIVAR P16S, augmented by data from 7°S to 7°N (Rafter et al., 2012) and station ALOHA at 22.75°N (Sigman et al., 2009)—to explore subsurface patterns in the nitrate isotopes, which they found to be strongly influenced by N cycle processes occurring in overlying surface waters. For instance, partial nitrate assimilation in Southern Ocean surface waters yields sinking PON that is relatively low in $\delta^{15}N$ compared to the background nitrate. As a result, subsurface nitrate, particularly in the Subantarctic, has a low $\delta^{15}N$ for its $\delta^{18}O$ (Rafter et al., 2013; Fripiat et al., 2019, 2021a). The subsequent subduction and northward advection of the partially assimilated surface nitrate in AAIW and the less dense SAMW means that thermocline nitrate sourced from the Southern Ocean is relatively high in $\delta^{15}N$

(Sigman et al., 2000, 2009; DiFiore et al., 2006; Rafter et al., 2013; Marconi et al., 2015). The upward supply and consumption of this high-$\delta^{15}N$ nitrate in the low-latitude surface yields sinking PON that is as high or higher in $\delta^{15}N$ than the subsurface water mass into which it is remineralized, causing the $\delta^{15}N$ of subsurface nitrate to be elevated relative to its $\delta^{18}O$ (Rafter et al., 2013). This trend is eroded in the western Pacific, North Atlantic, and southwest Indian subtropical gyres where the remineralization of low-$\delta^{15}N$ material causes the $\delta^{15}N$ of thermocline nitrate to decrease considerably more than its $\delta^{18}O$ (Bock et al., 1989; Knapp et al., 2008; Rafter et al., 2013; Marconi et al., 2015, 2017b; Forrer et al., 2023; Marshall et al., 2023). In nitrate $\delta^{18}O$ versus $\delta^{15}N$ space, N_2 fixation drives thermocline nitrate towards a $\delta^{15}N$ of –1‰ and $\delta^{18}O$ of +1.1‰, the values expected for the nitrification of newly fixed N (orange arrow in Figure 6c; Knapp et al., 2008).

Estimating the $\delta^{15}N$ of sinking PON from nitrate isotope sections has implications for determining the extent to which surface productivity is fueled by N_2 fixation versus subsurface nitrate (Altabet, 1988; Casciotti et al., 2008; Rafter et al., 2013; Marconi et al., 2019) and for understanding the influence of denitrification in the Pacific ODZs on basin-scale biogeochemistry (Figure 7a; Rafter et al., 2013; Peters et al., 2018b). However, the preferential consumption of ^{14}N-bearing (and/or low-$\delta^{15}N$) forms of DON and/or suspended PON may also contribute to the accumulation of low-$\delta^{15}N$ nitrate in the upper thermocline (Casciotti et al., 2008; Knapp et al., 2018; Zhang et al., 2020) and would have a similar effect on thermocline nitrate isotopes to that of remineralization of N_2 fixation-sourced sinking PON described above.

Deman et al. (2021) measured the nitrate isotopes along GA01 (40°–60°N, 12°–54°W) to the north of GA03, sampling both the subtropical and subpolar North Atlantic. They concluded from the cohesive relationship of nitrate concentration to $\delta^{15}N$ that nitrate is supplied to the subpolar gyre surface from the upward mixing of Labrador Sea Water, then consumed as the Ekman layer flows equatorward. In addition, at the base of the deep mixed layer of the subpolar gyre, the rise in nitrate $\delta^{18}O$ coincident with no change in its $\delta^{15}N$ indicates coupled partial nitrate assimilation and nitrification (as exemplified by the magenta arrow in Figure 6c; Sigman et al., 2005; Fawcett et al., 2015). The nitrate sections show that this signal is transported into the subtropical thermocline via the subduction and equatorward flow of isopycnals

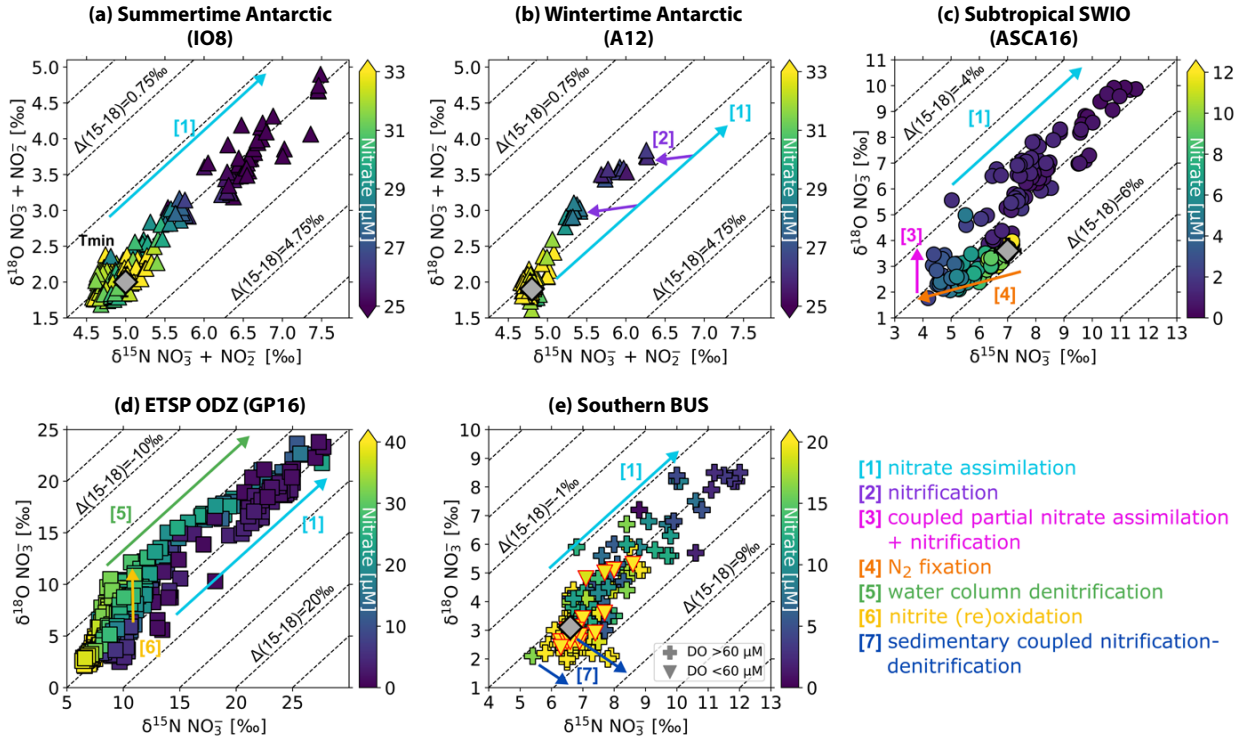

FIGURE 6. Nitrate $\delta^{18}O$ (‰ vs. VSMOW) versus $\delta^{15}N$ (‰ vs. air) for the (a) summertime Antarctic (IO8) (Fripiat et al., 2019), (b) wintertime Antarctic (A12) (Smart et al., 2015), (c) subtropical southwest Indian Ocean (ASCA16) (Marshall et al., 2023), (d) Eastern Tropical South Pacific (GP16) (Peters et al., 2018b), and (e) southern Benguela upwelling system (SBUS) (Flynn et al., 2020). Symbol color shows sample nitrate concentration, and the effect of the major N cycle processes on the nitrate isotopes is indicated by the arrows (see legend). Dashed contour lines show Δ(15-18) [(‰) = $\delta^{15}N$ – $\delta^{18}O$] (Sigman et al., 2005; Rafter et al., 2013). The gray diamonds on panels a and b indicate the mean $\delta^{18}O$ and $\delta^{15}N$ of nitrate in Circumpolar Deep Water (CDW), and those on panels c and e, of nitrate in Subantarctic Mode Water (SAMW); these water masses constitute the ultimate source of nutrients to the surface layer of the Antarctic and subtropical southwest Indian Ocean and SBUS, respectively (Sigman et al., 2000; Flynn et al., 2020; Marshall et al., 2023). In panel e, samples with dissolved oxygen concentrations (DO) <60 μM are distinguished by triangles.

that outcrop in the subpolar region. The authors conclude that repeated cycles of nitrate consumption and nitrification act to drive down the $\delta^{18}O$ of nitrate in the east-to-west flowing thermocline waters of the subtropical gyre, with nitrate eventually converging on the low $\delta^{18}O$ (1.1‰; essentially the nitrification value) observed at the Bermuda Atlantic Time-series Study site (Knapp et al., 2008; Fawcett et al., 2015, 2018). The same remineralization pathways also cause the $\delta^{15}N$ of subtropical North Atlantic thermocline nitrate to decline as newly fixed nitrate is added (Knapp et al., 2008; Bourbonnais et al., 2009; Marconi et al., 2015).

Lehmann et al. (2019) measured the nitrate isotopes along line GN02 that transects the Labrador Sea, Baffin Bay, and the Canadian Arctic Archipelago. In Baffin Bay, the high $\delta^{15}N$ (7‰) and low $\delta^{18}O$ (1‰) of deep-water nitrate suggest a Pacific origin for the nutrients that ultimately support export production. Because the lower $\delta^{15}N$ (5.8‰) of nitrate in the overlying intermediate waters evinces a contribution of Atlantic water, and given that less sinking material will be remineralized in deep than intermediate waters, the authors conclude that the deep basin residence time must be much longer than that of the intermediate layer. The implication is that nutrients removed from Baffin Bay surface waters are trapped at depth over long timescales. By combining their nitrate isotope data (invariant $\delta^{15}N$ and $\delta^{18}O$ at depth) with N* (<–4 µM), N. Lehmann et al. (2019) also determine that sedimentary denitrification is a substantial sink for fixed N in Baffin Bay.

UNDERSTANDING NITROGEN CYCLING AND LOSS IN OXYGEN DEFICIENT ZONES

The quantity of fixed N loss from the ocean has been widely documented through the distributions of oxygen and nutrients (nitrate and phosphate). For example, nitrate deficits were used to estimate the quantity and rate of N loss in the low oxygen waters of the ETNP (Cline and Richards, 1972). N* has also been used to estimate the Pacific N budget (Deutsch et al., 2001). This approach yielded rates of water column denitrification in the ETNP and ETSP of 22 ± 3.4 and 26 ± 4.1 Tg N yr^{-1}, respectively. While N* inherently makes assumptions about the N:P stoichiometry of organic matter and the mechanism of N loss, these estimates are remarkably similar to those based on the distributions of excess N_2, which are independent of N:P remineralization ratios and N loss mechanisms (Chang et al., 2010; DeVries et al., 2012, 2013). Global models that allow variation in the N:P of exported organic matter also yield similar rates of water column N loss in the Pacific (Wang et al., 2019).

Nitrate isotope measurements have provided additional insights into N cycling and loss in water column ODZs (Sigman et al., 2005; Casciotti, 2016b). As nitrate is consumed by denitrification, preferential removal of ^{14}N-nitrate leads to progressive enrichment of ^{15}N in the remaining nitrate pool (green arrow in Figure 6d). This isotopic fractionation is clearly observed in marine ODZs (Figure 7a) and has been quantified as an isotope effect, which relates a given increase in $\delta^{15}N$ or $\delta^{18}O$ to the amount of nitrate removed (Mariotti et al., 1981). In order to translate nitrate isotope measurements into a quantity of N loss, it is important to know this conversion factor (isotope effect) accurately. However, estimates of the isotope effect range from 13‰ to 40‰ for water column denitrification (Cline and Kaplan, 1975; Brandes et al., 1998; Voss et al., 2001) and 0‰–3‰ for benthic denitrification (Brandes and Devol, 1997; M.F. Lehmann et al., 2007; Somes et al., 2013), with differing implications for the fraction of N loss occurring in the water column versus the sediments and the overall amount of N lost from the ocean. For example, using an isotope effect for water column denitrification of 25‰ to evaluate the marine N isotope budget, sedimentary denitrification is required to exceed water column denitrification by a factor of 3 to 4 (Brandes and Devol, 2002). This magnitude of sedimentary denitrification, however, results in a significant imbalance in the global marine N budget (Codispoti, 2007).

Subsequent work has shown that processes other than denitrification are important to consider in the N cycle

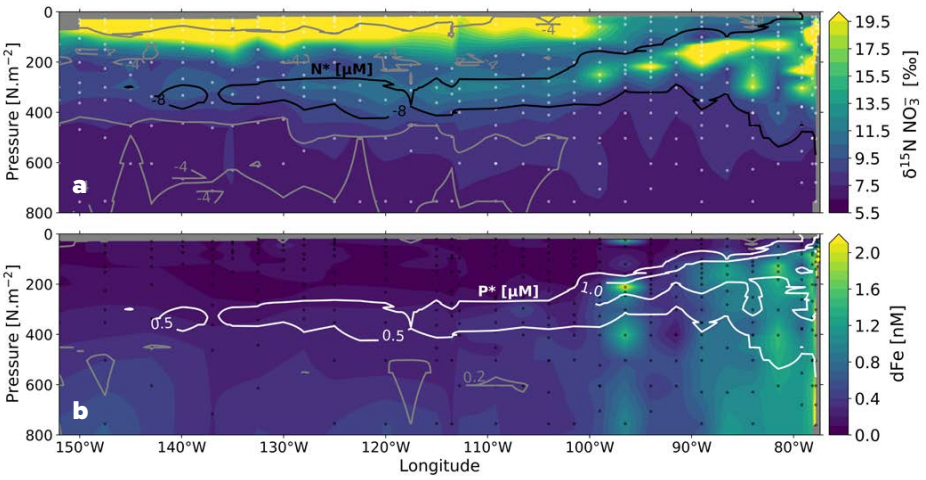

FIGURE 7. Zonal depth sections across the eastern tropical South Pacific Ocean (GP16 along ~15°S) of (a) nitrate $\delta^{15}N$ (‰ vs. air) (Peters et al., 2018b) with black and gray contours indicating N* (= $[NO_3^-]$ – 16 × $[PO_4^{3-}]$) (µM), and (b) dissolved iron (dFe) (nM) (GEOTRACES Intermediate Data Product Group, 2023) with white and gray contours indicating P* (= $[PO_4^{3-}]$ – $[NO_3^-]$ ÷ 16) (µM). On panel a, high-$\delta^{15}N$ nitrate and low N* result from water column denitrification, the signal of which is advected westward from the eastern tropical South Pacific low oxygen margin. On panel b, elevated dissolved iron concentrations supplied by the margin overlap with elevated P*, which together could promote N_2 fixation in the nearshore waters.

of marine ODZs. Anammox (Kuypers et al., 2005; Lam et al., 2009; Ward, 2013; Babbin et al., 2014), nitrite (re)oxidation (i.e., the oxidation of nitrite produced via dissimilatory nitrate reduction in the ODZ; Fussel et al., 2012; Casciotti, 2016a), and migration of zooplankton (Bianchi et al., 2014) can contribute to the speciation, quantity, and isotopic composition of fixed N species and subsequent marine N loss. In particular, the isotope effect for denitrification could be overestimated based on water column nitrate isotope measurements due to two factors linked to nitrite oxidation: (1) the nitrate deficit does not accurately reflect the amount of nitrate reduction that has occurred (i.e., if most of the nitrate reduced to nitrite is subsequently reoxidized, it does not contribute to the nitrate deficit), and (2) the ^{15}N enrichment in nitrate is amplified through the inverse kinetic isotope effect for nitrite oxidation, which causes nitrite enriched in ^{15}N to be preferentially reoxidized to nitrate (yellow arrow in Figure 6d; Casciotti, 2009; Casciotti et al., 2013; Gaye et al., 2013; Bourbonnais et al., 2015; Peters et al., 2018a). A widespread influence of nitrite oxidation in marine ODZs (T.S. Martin et al., 2019a; Babbin et al., 2020; Buchanan et al., 2023; Sun et al., 2023) thus suggests that the isotope effect for water column denitrification is likely lower than 25‰, which would require less benthic denitrification to balance the N isotope budget.

Further insights into the isotope effects for water column denitrification come from sectional studies and large-scale data analyses (Marconi et al., 2017a; Peters et al., 2018b). Marconi et al. (2017a) compared the results of a multibox model involving aerobic respiration and denitrification to nitrate isotope measurements along isopycnal surfaces across the South Pacific. They observed that as the $\delta^{15}N$ of nitrate increases along isopycnal surfaces, its concentration also increases. They modeled the increases in nitrate concentration and $\delta^{15}N$ arising from the combination of aerobic remineralization, which produces nitrate with a $\delta^{15}N$ reflecting that of the biomass being degraded, and denitrification, which consumes nitrate and raises the $\delta^{15}N$ of the residual nitrate pool. From this analysis, an isotope effect for denitrification as low as 13‰ was found to fit the nitrate isotope data, which is in keeping with studies of denitrifying bacteria grown under conditions (i.e., organic matter and nitrate supplies) similar to those found in the ocean (Kritee et al., 2012), and could allow a nitrate mass and isotope budget that is balanced (DeVries et al., 2012).

The influence of ODZ processes on nitrate isotope distributions was also examined in the South Pacific along the GEOTRACES GP16 section between Peru and Tahiti (Peters et al., 2018b). Coincident measurements of nitrate isotopes (Figure 7a; Peters et al., 2018b) and dissolved iron (Figure 7b; GEOTRACES Intermediate Data Product Group, 2023) on this GEOTRACES section also provided insights into potential limitation of N_2 fixation by iron in the subtropical gyre. Surface samples with low nitrate and iron concentrations appear to be affected primarily by nitrate assimilation, without clear effects of N_2 fixation (Peters et al., 2018b). In contrast, the samples from the ODZ have higher nitrate concentrations and are impacted by a combination of water column denitrification and nitrite reoxidation (Figure 6d; Casciotti and Buchwald, 2012). Using an isotope mixing model, the contributions of preformed, regenerated, and ODZ-derived nitrate to the distribution of nitrate isotopes along the section were also determined. Both denitrification and remineralization of high-$\delta^{15}N$ organic matter likely contribute to elevating nitrate $\delta^{15}N$ above the preformed values imported from the Southern Ocean (Rafter et al., 2013). This interpretation supports that of Marconi et al. (2017a), who found that by including remineralized nitrate, the nitrate isotope distributions could be explained by a 13‰ isotope effect for water column denitrification. T.S. Martin et al. (2019b) also found that a lower isotope effect for denitrification (13‰) was suitable for simulating nitrate $\delta^{15}N$ values observed in and around ODZs using a 3D global inverse model (T.S. Martin et al., 2019a).

Shorter, more spatially resolved nitrate isotope sections have also proven valuable in regions where the biogeochemical and physical variability is high. For example, Flynn et al. (2020) measured the nitrate isotope ratios along four zonal transects (extending ≤300 km offshore and comprising at least 10 stations each) of the southern Benguela upwelling system (SBUS). Here, wind-driven upwelling of offshore SAMW occurs in spring and summer, with quiescent conditions prevailing in autumn and winter (Hutchings et al., 2009). Primary productivity in SBUS surface waters is remarkably high, exceeding that which can be supported by the offshore SAMW nutrient supply. Flynn et al. (2020) found in both summer and winter that regenerated nitrate and phosphate were "trapped" on the shelf, significantly augmenting the nutrient reservoir available for upwelling. Moreover, this subsurface nitrate was high in $\delta^{15}N$ and low in $\delta^{18}O$ relative to off-shelf SAMW, the bottom waters were characterized by a significant N deficit (shelf-wide mean of 4.6–6.0 µM; individual values as high as 23 µM), and oxygen concentrations were typically >60 µM. These data are best explained by coupled nitrification-denitrification in the sediments, which drives the loss of low-$\delta^{15}N$ N_2 and raises the $\delta^{15}N$ of the fixed N remaining in the water column, while concurrently decreasing its $\delta^{18}O$ (blue arrows in Figure 6e; Granger et al., 2011; Brown et al., 2015). Similar relationships of nitrate $\delta^{15}N$ to $\delta^{18}O$ and N deficit have been observed on the Bering Sea and Chukchi shelves in the Arctic (Granger et al., 2011, 2013; Fripiat et al., 2018). In the SBUS, Flynn et al. (2020) also observed a few incidences of nitrate $\delta^{15}N$ and $\delta^{18}O$ rising in concert for subsurface samples characterized by the lowest oxygen concentrations, consistent with water column denitrification (triangles in Figure 6e; that these data do not fall along a slope of 1:1 and are

not characterized by a lower dissolved oxygen concentration can be explained by on-shelf mixing with higher-oxygen waters containing nitrate with a different relationship of $\delta^{18}O$ to $\delta^{15}N$). In the SBUS, therefore, the dual nitrate isotopes yield insights into oxygen conditions because denitrification (coincident rise in $\delta^{15}N$ and $\delta^{18}O$) requires water column suboxia whereas coupled nitrification-denitrification ($\delta^{15}N$ rise and $\delta^{18}O$ decline) signals the development of suboxia in the sediments. The former scenario indicates a loss of N availability in the water column, with negative implications for higher trophic levels including fish, while the latter is most deleterious for benthic species.

LOOKING AHEAD

The increasing availability of isotope measurements of nitrate and DON lends itself to interpretation using regional-, basin-, and global-scale model frameworks. Modeling of nitrate isotopes has already enabled significant advances in our understanding of the inputs, outputs, and internal cycling of N in the ocean (Somes et al., 2010; DeVries et al., 2013; Yang and Gruber, 2016; Martin et al., 2019b; Rafter et al., 2019; Fripiat et al., 2021a, 2023). For example, the sensitivity of deep ocean nitrate $\delta^{15}N$ to surface productivity and ocean circulation (Fripiat et al., 2023) implies that past changes in deep nitrate $\delta^{15}N$ may not have been entirely due to variations in the fixed N budget (Brandes and Devol, 2002; Deutsch et al., 2004; Fripiat et al., 2023), particularly given likely changes in both productivity and circulation (Sigman et al., 2010). Further improvements in the spatial and temporal coverage of N isotope measurements will continue to constrain N cycle processes and their variability across seasons and ocean basins with differing circulation, productivity, ventilation rates, trace metal availability, and patterns of net N input or loss. In particular, we anticipate additional data from the Pacific and Indian Oceans from GEOTRACES cruises and analyses still underway. Moreover, the incorporation of rapidly growing N isotope databases (e.g., Figure 2, as well as DON $\delta^{15}N$) into coupled biogeochemical ocean models will improve coherent quantification and characterization of rates, transformations, and isotope effects for N cycle processes needed to reproduce these expanding data on a global scale.

SUPPLEMENTARY MATERIALS

Table S1 is available online at https://doi.org/10.5670/oceanog.2024.406.

REFERENCES

Altabet, M.A. 1988. Variations in nitrogen isotopic composition between sinking and suspended particles: Implications for nitrogen cycling and particle transformation in the open ocean. *Deep Sea Research Part I* 35:535–554, https://doi.org/10.1016/0198-0149(88)90130-6.

Altabet, M.A. 2001. Nitrogen isotopic evidence for micronutrient control of fractional NO_3^- utilization in the equatorial Pacific. *Limnology and Oceanography* 46(2):368–380, https://doi.org/10.4319/lo.2001.46.2.0368.

Altieri, K.E., S.E. Fawcett, and M.G. Hastings. 2021. Reactive nitrogen cycling in the atmosphere and ocean. *Annual Review of Earth and Planetary Sciences* 49(1):523–550, https://doi.org/10.1146/annurev-earth-083120-052147.

Arrigo, K.R. 2005. Marine microorganisms and global nutrient cycles. *Nature* 437(7057):349–355, https://doi.org/10.1038/nature04159.

Babbin, A.R., R.G. Keil, A.H. Devol, and B.B. Ward. 2014. Organic matter stoichiometry, flux, and oxygen control nitrogen loss in the ocean. *Science* 344(6182):406–408, https://doi.org/10.1126/science.1248364.

Babbin, A.R., C. Buchwald, F.M.M. Morel, S.D. Wankel, and B.B. Ward. 2020. Nitrite oxidation exceeds reduction and fixed nitrogen loss in anoxic Pacific waters. *Marine Chemistry* 224:103814, https://doi.org/10.1016/j.marchem.2020.103814.

Beck, A.J., Y. Tsukamoto, A. Tovar-Sanchez, M. Huerta-Diaz, H.J. Bokuniewicz, and S.A. Sanudo-Wilhelmy. 2007. Importance of geochemical transformations in determining submarine groundwater discharge-derived trace metal and nutrient fluxes. *Applied Geochemistry* 22(2):477–490, https://doi.org/10.1016/j.apgeochem.2006.10.005.

Beck, A.J., J.K. Cochran, and S.A. Sañudo-Wilhelmy. 2010. The distribution and speciation of dissolved trace metals in a shallow subterranean estuary. *Marine Chemistry* 121(1-4):145–156, https://doi.org/10.1016/j.marchem.2010.04.003.

Berelson, W.M., W.Z. Haskell, M. Prokopenko, A.N. Knapp, D.E. Hammond, N. Rollins, and D.G. Capone. 2015. Biogenic particle flux and benthic remineralization in the Eastern Tropical South Pacific. *Deep Sea Research Part I* 99:23–34, https://doi.org/10.1016/j.dsr.2014.12.006.

Berman-Frank, I., J.T. Cullen, Y. Shaked, R.M. Sherrell, and P.G. Falkowski. 2001. Iron availability, cellular iron quotas, and nitrogen fixation in *Trichodesmium*. *Limnology and Oceanography* 46(6):1,249–1,260, https://doi.org/10.4319/lo.2001.46.6.1249.

Bianchi, D., A.R. Babbin, and E.D. Galbraith. 2014. Enhancement of anammox by the excretion of diel vertical migrators. *Proceedings of the National Academy of Sciences of the United States of America* 111(44):15,653–15,658, https://doi.org/10.1073/pnas.1410790111.

Bock, E., H.-P. Koops, and H. Harms. 1989. Nitrifying bacteria. Pp. 81–96 in *Autotrophic Bacteria*. H.G. Schelgel and B. Bowien, eds, Springer-Verlag, Berlin.

Bonnet, S., H. Berthelot, K. Turk-Kubo, S. Fawcett, E. Rahav, S. L'Helguen, and I. Berman-Frank. 2016. Dynamics of N_2 fixation and fate of diazotroph-derived nitrogen during the VAHINE mesocosm experiment. *Biogeosciences* 13:2,653–2,673, https://doi.org/10.5194/bg-13-2653-2016.

Bonnet, S., M. Caffin, H. Berthelot, and T. Moutin. 2017. Hot spot of N_2 fixation in the western tropical South Pacific pleads for a spatial decoupling between N_2 fixation and denitrification. *Proceedings of the National Academy of Sciences of the United States of America* 114(14):E2800–E2801, https://doi.org/10.1073/pnas.1619514114.

Bonnet, S., C. Guieu, V. Taillandier, C. Boulart, P. Bouruet-Aubertot, F. Gazeau, C. Scalabrin, M. Bressac, A.N. Knapp, Y. Cuypers, and others. 2023. Natural iron fertilization by shallow hydrothermal sources fuels diazotroph blooms in the ocean. *Science* 380(6647):812–817, https://doi.org/10.1126/science.abq4654.

Boshers, D.S., J. Granger, C.R. Tobias, J.K. Böhlke, and R.L. Smith. 2019. Constraining the oxygen isotopic composition of nitrate produced by nitrification. *Environmental Science & Technology* 53(3):1,206–1,216, https://doi.org/10.1021/acs.est.8b03386.

Bourbonnais, A., M.F. Lehmann, J.J. Waniek, and D.E. Schulz-Bull. 2009. Nitrate isotope anomalies reflect N_2 fixation in the Azores Front region (subtropical NE Atlantic). *Journal of Geophysical Research* 114(C3), https://doi.org/10.1029/2007JC004617.

Bourbonnais, A., M.A. Altabet, C.N. Charoenpong, J. Larkum, H. Hu, H.W. Bange, and L. Stramma. 2015. N-loss isotope effects in the Peru oxygen minimum zone studied using a mesoscale eddy as a natural tracer experiment. *Global Biogeochemical Cycles* 29(6):793–811, https://doi.org/10.1002/2014GB005001.

Boyd, P.W., and M.J. Ellwood. 2010. The biogeochemical cycle of iron in the ocean. *Nature Geoscience* 3(10):675–682, https://doi.org/10.1038/ngeo964.

Brandes, J.A., and A.H. Devol. 1997. Isotopic fractionation of oxygen and nitrogen in coastal marine sediments. *Geochimica et Cosmochimica Acta* 61(9):1,793–1,801, https://doi.org/10.1016/S0016-7037(97)00041-0.

Brandes, J.A., A.H. Devol, T. Yoshinari, D.A. Jayakumar, and S.W.A. Naqvi. 1998. Isotopic composition of nitrate in the central Arabian Sea and eastern tropical North Pacific: A tracer for mixing and nitrogen cycles. *Limnology and Oceanography* 43(7):1,680–1,689, https://doi.org/10.4319/lo.1998.43.7.1680.

Brandes, J.A., and A.H. Devol. 2002. A global marine fixed nitrogen isotopic budget: Implications for Holocene nitrogen cycling. *Global Biogeochemical Cycles* 16(4):67-1–67-14, https://doi.org/10.1029/2001gb001856.

Bronk, D.A., and B.B. Ward. 1999. Gross and net nitrogen uptake and DON release in the euphotic zone of Monterey Bay, California. *Limnology and Oceanography* 44:573–585, https://doi.org/10.4319/lo.1999.44.3.0573.

Bronk, D.A., and B.B. Ward. 2000. Magnitude of dissolved organic nitrogen release relative to gross nitrogen uptake in marine systems. *Limnology and Oceanography* 45(8):1,879–1,883, https://doi.org/10.4319/lo.2000.45.8.1879.

Brown, Z.W., K.L. Casciotti, R.S. Pickart, J.H. Swift, and K.R. Arrigo. 2015. Aspects of the marine nitrogen cycle of the Chukchi Sea shelf and Canada Basin. *Deep-Sea Research Part II* 118:73–87, https://doi.org/10.1016/j.dsr2.2015.02.009.

Bryant-Mason, A., Y.J. Xu, and M. Altabet. 2013. Isotopic signature of nitrate in river waters of the lower Mississippi and its distributary, the Atchafalaya. *Hydrological Processes* 27(19):2,840–2,850, https://doi.org/10.1002/hyp.9420.

Buchanan, P.J., X. Sun, J.L. Weissman, and E. Zakem. 2023. Oxygen intrusions sustain aerobic nitrite oxidation in anoxic marine zones. *bioRxiv*, https://doi.org/10.1101/2023.02.22.529547.

Buchwald, C., A.E. Santoro, M.R. McIlvin, and K.L. Casciotti. 2012. Oxygen isotopic composition of nitrate and nitrite produced by nitrifying cocultures and natural marine assemblages. *Limnology and Oceanography* 57(5):1,361–1,375, https://doi.org/10.4319/lo.2012.57.5.1361.

Capone, D.G., M.D. Ferrier, and E.J. Carpenter. 1994. Amino-acid cycling in colonies of the planktonic marine cyanobacterium *Trichodesmium thiebautii*. *Applied and Environmental Microbiology* 60(11):3,989–3,995, https://doi.org/10.1128/aem.60.11.3989-3995.1994.

Capone, D.G., M. Subramaniam, J.P. Montoya, M. Voss, C. Humborg, A.M. Johansen, R.L. Siefert, and E.J. Carpenter. 1998. An extensive bloom of N_2-fixing cyanobacterium *Trichodesmium erythraeum* in the central Arabian Sea. *Marine Ecology-Progress Series* 172:237–281, https://doi.org/10.7916/D8416X1H.

Carpenter, E.J., H.R. Harvey, B. Fry, and D.G. Capone. 1997. Biogeochemical tracers of the marine cyanobacterium Trichodesmium. *Deep Sea Research Part I* 44(1):27–38, https://doi.org/10.1016/S0967-0637(96)00091-X.

Casciotti, K.L., D.M. Sigman, M.G. Hastings, J.K. Böhlke, and A. Hilkert. 2002. Measurement of the oxygen isotopic composition of nitrate in seawater and freshwater using the denitrifier method. *Analytical Chemistry* 74(19):4,905–4,912, https://doi.org/10.1021/ac020113w.

Casciotti, K.L., T.W. Trull, D.M. Glover, and D. Davies. 2008. Constraints on nitrogen cycling in the subtropical North Pacific Station ALOHA from isotopic measurements of nitrate and particulate nitrogen. *Deep Sea Research II* 55:1,661–1,672, https://doi.org/10.1016/j.dsr2.2008.04.017.

Casciotti, K.L. 2009. Inverse kinetic isotope fractionation during bacterial nitrite oxidation. *Geochimica et Cosmochimica Acta* 73(7):2,061–2,076, https://doi.org/10.1016/j.gca.2008.12.022.

Casciotti, K.L., and C. Buchwald. 2012. Insights on the marine microbial nitrogen cycle from isotopic approaches to nitrification. *Frontiers in Microbiology* 3:356, https://doi.org/10.3389/fmicb.2012.00356.

Casciotti, K.L., C. Buchwald, and M. McIlvin. 2013. Implications of nitrate and nitrite isotopic measurements for the mechanisms of nitrogen cycling in the Peru oxygen deficient zone. *Deep-Sea Research Part I* 80:78–93, https://doi.org/10.1016/j.dsr.2013.05.017.

Casciotti, K.L. 2016a. Nitrite isotopes as tracers of marine N cycle processes. *Philosophical Transactions of the Royal Society A* 374(2081), https://doi.org/10.1098/rsta.2015.0295.

Casciotti, K.L. 2016b. Nitrogen and oxygen isotopic studies of the marine nitrogen cycle. *Annual Review of Marine Science* 8:379–407, https://doi.org/10.1146/annurev-marine-010213-135052.

Chang, B.X., A.H. Devol, and S.R. Emerson. 2010. Denitrification and the nitrogen gas excess in the eastern tropical South Pacific oxygen deficient zone. *Deep Sea Research Part I* 57(9):1,092–1,101, https://doi.org/10.1016/j.dsr.2010.05.009.

Chen, X., H.K. Kwon, D. Joung, C. Baek, T.G. Park, M. Son, and G. Kim. 2022. Role of terrestrial versus marine sources of humic dissolved organic matter on the behaviors of trace elements in seawater. *Geochimica et Cosmochimica Acta* 333:333–346, https://doi.org/10.1016/j.gca.2022.07.025.

Chen, X.-G., D. Rusiecka, M. Gledhill, A. Milne, A.L. Annett, A.J. Birchill, M.C. Lohan, S. Ussher, E.M.S. Woodward, and E.P. Achterberg. 2023. Ocean circulation and biological processes drive seasonal variations of dissolved Al, Cd, Ni, Cu, and Zn on the Northeast Atlantic continental margin. *Marine Chemistry* 252:104246, https://doi.org/10.1016/j.marchem.2023.104246.

Chowdhury, S., E. Raes, C. Hörstmann, A. Ahmed, C. Ridame, N. Metzl, P.S. Bhavya, T. Sato, T. Shiozaki, S. Bonnet, and others. 2023. Diazotrophy in the Indian Ocean: Current understanding and future perspectives. *Limnology and Oceanography Letters* 8(5):707–722, https://doi.org/10.1002/lol2.10343.

Cline, J.D., and F.A. Richards. 1972. Oxygen deficient conditions and nitrate reduction in the Eastern Tropical North Pacific Ocean. *Limnology and Oceanography* 17(6):885–900, https://doi.org/10.4319/lo.1972.17.6.0885.

Cline, J.D., and I.R. Kaplan. 1975. Isotopic fractionation of dissolved nitrate during denitrification in the eastern tropical North Pacific Ocean. *Marine Chemistry* 3:271–299, https://doi.org/10.1016/0304-4203(75)90009-2.

Codispoti, L.A. 2007. An oceanic fixed nitrogen sink exceeding 400 Tg N a^{-1} vs the concept of homeostasis in the fixed-nitrogen inventory. *Biogeosciences* 4(2):233–253, https://doi.org/10.5194/bg-4-233-2007.

Conway, T.M., and S.G. John. 2014. Quantification of dissolved iron sources to the North Atlantic Ocean. *Nature* 511(7508):212–215, https://doi.org/10.1038/nature13482.

Dekaezemacker, J., S. Bonnet, O. Grosso, T. Moutin, M. Bressac, and D.G. Capone. 2013. Evidence of active dinitrogen fixation in surface waters of the eastern tropical South Pacific during El Niño and La Niña events and evaluation of its potential nutrient controls. *Global Biogeochemical Cycles* 27(3):768–779, https://doi.org/10.1002/gbc.20063.

Deman, F., D. Fonseca-Batista, A. Roukaerts, M.I. García-Ibáñez, E. Le Roy, E.P.D.N. Thilakarathne, M. Elskens, F. Dehairs, and F. Fripiat. 2021. Nitrate supply routes and impact of internal cycling in the North Atlantic Ocean inferred from nitrate isotopic composition. *Global Biogeochemical Cycles* 35(4):e2020GB006887, https://doi.org/10.1029/2020GB006887.

Deutsch, C., N. Gruber, R.M. Key, J.L. Sarmiento, and A. Ganaschaud. 2001. Denitrification and N_2 fixation in the Pacific Ocean. *Global Biogeochemical Cycles* 15(2):483–506, https://doi.org/10.1029/2000GB001291.

Deutsch, C., D.M. Sigman, R.C. Thunell, A.N. Meckler, and G.H. Haug. 2004. Isotopic constraints on glacial/interglacial changes in the oceanic nitrogen budget. *Global Biogeochemical Cycles* 18(4), https://doi.org/10.1029/2003GB002189.

Deutsch, C., J.L. Sarmiento, D.M. Sigman, N. Gruber, and J.P. Dunne. 2007. Spatial coupling of nitrogen inputs and losses in the ocean. *Nature* 445:163–167, https://doi.org/10.1038/nature05392.

DeVries, T., C. Deutsch, F. Primeau, B. Chang, and A. Devol. 2012. Global rates of water-column denitrification derived from nitrogen gas measurements. *Nature Geoscience* 5(8):547–550, https://doi.org/10.1038/ngeo1515.

DeVries, T., C. Deutsch, P.A. Rafter, and F. Primeau. 2013. Marine denitrification rates determined from a global 3-D inverse model. *Biogeosciences* 10(4):2,481–2,496, https://doi.org/10.5194/bg-10-2481-2013.

DiFiore, P.J., D.M. Sigman, T.W. Trull, M.J. Lourey, K.L. Karsh, G. Cane, and R. Ho. 2006. Nitrogen isotope constraints on subantarctic biogeochemistry. *Journal of Geophysical Research: Oceans* 111(C8), https://doi.org/10.1029/2005jc003216.

Duce, R.A., P.S. Liss, J.T. Merrill, E.L. Atlas, P. Buat-Menard, B.B. Hicks, J.M. Miller, J.M. Prospero, R. Arimoto, T.M. Church, and others. 1991. The atmospheric input of trace species to the world ocean. *Global Biogeochemical Cycles* 5(3):193–259, https://doi.org/10.1029/91GB01778.

Dugdale, R.C., and J.J. Goering. 1967. Uptake of new and regenerated forms of nitrogen in marine production. *Limnology and Oceanography* 12:196–206, https://doi.org/10.4319/lo.1967.12.2.0196.

Duhamel, S., J.M. Diaz, J.C. Adams, K. Djaoudi, V. Steck, and E.M. Waggoner. 2021. Phosphorus as an integral component of global marine biogeochemistry. *Nature Geoscience* 14(6):359–368, https://doi.org/10.1038/s41561-021-00755-8.

Dupont, C.L., K. Barbeau, and B. Palenik. 2008. Ni uptake and limitation in marine *Synechococcus* strains. *Applied and Environmental Microbiology* 74(1):23–31, https://doi.org/10.1128/AEM.01007-07.

Dyhrman, S.T., and K.C. Ruttenberg. 2006. Presence and regulation of alkaline phosphatase activity in eukaryotic phytoplankton from the coastal ocean: Implications for dissolved organic phosphorus remineralization. *Limnology and Oceanography* 51(3):1,381–1,390, https://doi.org/10.4319/lo.2006.51.3.1381.

Eppley, R.W., and B.J. Peterson. 1979. Particulate organic matter flux and planktonic new production in the deep ocean. *Nature* 282:677–680, https://doi.org/10.1038/282677a0.

Fawcett, S.E., B.B. Ward, M.W. Lomas, and D.M. Sigman. 2015. Vertical decoupling of nitrate assimilation and nitrification in the Sargasso Sea. *Deep Sea Research Part I* 103:64–72, https://doi.org/10.1016/j.dsr.2015.05.004.

Fawcett, S.E., K.S. Johnson, S.C. Riser, N. Van Oostende, and D.M. Sigman. 2018. Low-nutrient organic matter in the Sargasso Sea thermocline: A hypothesis for its role, identity, and carbon cycle implications. *Marine Chemistry* 207:108–123, https://doi.org/10.1016/j.marchem.2018.10.008.

Ferguson, S.J., D.J. Richardson, and R.J.M. van Spanning. 2007. Biochemistry and molecular biology of nitrification. Pp. 209–222 in *Biology of the Nitrogen Cycle*. H. Bothe, S.J. Ferguson, and W.E. Newton, eds, Elsevier, Amsterdam, https://doi.org/10.1016/B978-044452857-5.50015-1.

Fernandez, C., L. Farias, and O. Ulloa. 2011. Nitrogen fixation in denitrified marine waters. *PLoS ONE* 6:e20539, https://doi.org/10.1371/journal.pone.0020539.

Fitzsimmons, J.N., S.G. John, C.M. Marsay, C.L. Hoffman, S.L. Nicholas, B.M. Toner, C.R. German, and R.M. Sherrell. 2017. Iron persistence in a distal hydrothermal plume supported by dissolved–particulate exchange. *Nature Geoscience* 10(3):195–201, https://doi.org/10.1038/ngeo2900.

Fitzsimmons, J.N., and T.M. Conway. 2023. Novel insights into marine iron biogeochemistry from iron isotopes. *Annual Review of Marine Science* 15(1):383–406, https://doi.org/10.1146/annurev-marine-032822-103431.

Flynn, R.F., J. Granger, J.A. Veitch, S. Siedlecki, J.M. Burger, K. Pillay, and S.E. Fawcett. 2020. On-shelf nutrient trapping enhances the fertility of the southern Benguela upwelling system. *Journal of Geophysical Research: Oceans* 125(6):e2019JC015948, https://doi.org/10.1029/2019JC015948.

Forrer, H.J., S. Bonnet, R.K. Thomas, O. Grosso, C. Guieu, and A.N. Knapp. 2023. Quantifying N_2 fixation and its contribution to export production near the Tonga-Kermadec Arc using nitrogen isotope budgets. *Frontiers in Marine Science* 10:1249115, https://doi.org/10.3389/fmars.2023.1249115.

Fripiat, F., M. Declercq, C.J. Sapart, L.G. Anderson, V. Bruechert, F. Deman, D. Fonseca-Batista, C. Humborg, A. Roukaerts, I.P. Semiletov, and F. Dehairs. 2018. Influence of the bordering shelves on nutrient distribution in the Arctic halocline inferred from water column nitrate isotopes. *Limnology and Oceanography* 63(5):2,154–2,170, https://doi.org/10.1002/lno.10930.

Fripiat, F., A. Martínez-García, S.E. Fawcett, P.C. Kemeny, A.S. Studer, S.M. Smart, F. Rubach, S. Oleynik, D.M. Sigman, and G.H. Haug. 2019. The isotope effect of nitrate assimilation in the Antarctic Zone: Improved estimates and paleoceanographic implications. *Geochimica et Cosmochimica Acta* 247:261–279, https://doi.org/10.1016/j.gca.2018.12.003.

Fripiat, F., A. Martínez-García, D. Marconi, S.E. Fawcett, S.H. Kopf, V.H. Luu, P.A. Rafter, R. Zhang, D.M. Sigman, and G.H. Haug. 2021a. Nitrogen isotopic constraints on nutrient transport to the upper ocean. *Nature Geoscience* 14(11):855–861, https://doi.org/10.1038/s41561-021-00836-8.

Fripiat, F., D. Marconi, P.A. Rafter, D.M. Sigman, M.A. Altabet, A. Bourbonnais, J. Brandes, K.K.L. Casciotti, F. Deman, F. Dehairs, and others. 2021b. Compilation of nitrate δ15N in the Ocean, https://doi.org/10.1594/PANGAEA.936484.

Fripiat, F., D.M. Sigman, A. Martínez-García, D. Marconi, X.E. Ai, A. Auderset, S.E. Fawcett, S. Moretti, A.S. Studer, and G.H. Haug. 2023. The impact of incomplete nutrient consumption in the Southern Ocean on global mean ocean nitrate $\delta^{15}N$. *Global Biogeochemical Cycles* 37(2):e2022GB007442, https://doi.org/10.1029/2022GB007442.

Fussel, J., P. Lam, G. Lavik, M.M. Jensen, M. Holtappels, M. Gunter, and M.M.M. Kuypers. 2012. Nitrite oxidation in the Namibian oxygen minimum zone. *The ISME Journal* 6:1,200–1,209, https://doi.org/10.1038/ismej.2011.178.

Gaye, B., B. Nagel, K. Dähnke, T. Rixen, and K.C. Emeis. 2013. Evidence of parallel denitrification and nitrite oxidation in the ODZ of the Arabian Sea from paired stable isotopes of nitrate and nitrite. *Global Biogeochemical Cycles* 27(4):1,059–1,071, https://doi.org/10.1002/2011GB004115.

GEOTRACES Intermediate Data Product Group. 2023. The GEOTRACES Intermediate Data Product 2021 version 2 (IDP2021v2), https://doi.org/10.5285/ff46f034-f47c-05f9-e053-6c86abc0dc7e.

Glibert, P.M., and D.A. Bronk. 1994. Release of dissolved organic nitrogen by marine diazotrophic cyanobacteria, *Trichodesmium* spp. *Applied and Environmental Microbiology* 60(11):3,996–4,000, https://doi.org/10.1128/aem.60.11.3996-4000.1994.

Grand, M.M., C.I. Measures, M. Hatta, P.L. Morton, P. Barrett, A. Milne, J.A. Resing, and W.M. Landing. 2015. The impact of circulation and dust deposition in controlling the distributions of dissolved Fe and Al in the south Indian subtropical gyre. *Marine Chemistry* 176:110–125, https://doi.org/10.1016/j.marchem.2015.08.002.

Granger, J., D.M. Sigman, J.A. Needoba, and P.J. Harrison. 2004. Coupled nitrogen and oxygen isotope fractionation of nitrate during assimilation by cultures of marine phytoplankton. *Limnology and Oceanography* 49(5):1,763–1,773, https://doi.org/10.4319/lo.2004.49.5.1763.

Granger, J., D.M. Sigman, M.F. Lehmann, and P.D. Tortell. 2008. Nitrogen and oxygen isotope fractionation during dissimilatory nitrate reduction by denitrifying bacteria. *Limnology and Oceanography* 53(6):2,533–2,545, https://doi.org/10.4319/lo.2008.53.6.2533.

Granger, J., D.M. Sigman, M.M. Rohde, M.T. Maldonado, and P.D. Tortell. 2010. N and O isotope effects during nitrate assimilation by unicellular prokaryotic and eukaryotic plankton cultures. *Geochimica et Cosmochimica Acta* 74:1,030–1,040, https://doi.org/10.1016/j.gca.2009.10.044.

Granger, J., M.G. Prokopenko, D.M. Sigman, C.W. Mordy, Z.M. Morse, L.V. Morales, R.N. Sambrotto, and B. Plessen. 2011. Coupled nitrification-denitrification in sediment of the eastern Bering Sea shelf leads to ^{15}N enrichment of fixed N in shelf waters. *Journal of Geophysical Research* 116(C11), https://doi.org/10.1029/2010JC006751.

Granger, J., M.G. Prokopenko, C.W. Mordy, and D.M. Sigman. 2013. The proportion of remineralized nitrate on the ice-covered eastern Bering Sea shelf evidenced from the oxygen isotope ratio of nitrate. *Global Biogeochemical Cycles* 27(3):962–971, https://doi.org/10.1002/gbc.20075.

Gruber, N., and J.L. Sarmiento. 1997. Global patterns of marine nitrogen fixation and denitrification. *Global Biogeochemical Cycles* 11:235–266, https://doi.org/10.1029/97GB00077.

Hansell, D.A., and C.A. Carlson. 1998. Net community production of dissolved organic carbon. *Global Biogeochemical Cycles* 12(3):443–453, https://doi.org/10.1029/98GB01928.

Hansell, D.A., C.A. Carlson, R.M.W. Amon, X.A. Alvarez-Salgado, Y. Yamashita, C. Romera-Castillo, and M.B. Bif. 2021. Compilation of dissolved organic matter (DOM) data obtained from global ocean observations from 1994 to 2021. Version 2 (NCEI Accession 0227166), NOAA National Centers for Environmental Information. Data set, https://doi.org/10.25921/s4f4-ye35.

Hatta, M., C.I. Measures, J. Wu, S. Roshan, J.N. Fitzsimmons, P. Sedwick, and P. Morton. 2015. An overview of dissolved Fe and Mn distributions during the 2010–2011 US GEOTRACES north Atlantic cruises: GEOTRACES GA03. *Deep Sea Research Part II* 116:117–129, https://doi.org/10.1016/j.dsr2.2014.07.005.

Held, N.A., E.A. Webb, M.M. McIlvin, D.A. Hutchins, N.R. Cohen, D.M. Moran, K. Kunde, M.C. Lohan, C. Mahaffey, E.M.S. Woodward, and M.A. Saito. 2020. Co-occurrence of Fe and P stress in natural populations of the marine diazotroph *Trichodesmium*. *Biogeosciences* 17(9):2,537–2,551, https://doi.org/10.5194/bg-17-2537-2020.

Holl, C.M., T.A. Villareal, C.D. Payne, T.D. Clayton, C. Hart, and J.P. Montoya. 2007. *Trichodesmium* in the western Gulf of Mexico: $^{15}N_2$-fixation and natural abundance stable isotopic evidence. *Limnology and Oceanography* 52(5):2,249–2,259, https://doi.org/10.4319/lo.2007.52.5.2249.

Homoky, W.B., T.M. Conway, S.G. John, D. König, F. Deng, A. Tagliabue, and R.A. Mills. 2021. Iron colloids dominate sedimentary supply to the ocean interior. *Proceedings of the National Academy of Sciences of the United States of America* 118(13):e2016078118, https://doi.org/10.1073/pnas.2016078118.

Horii, S., K. Takahashi, T. Shiozaki, S. Takeda, M. Sato, T. Yamaguchi, S. Takino, F. Hashihama, Y. Kondo, T. Takemura, and K. Furuya. 2023. East-west variabilities of N_2 fixation activity in the subtropical North Pacific Ocean in summer: Potential field evidence of the phosphorus and iron co-limitation in the western area. *Journal of Geophysical Research: Oceans* 128(6):e2022JC019249, https://doi.org/10.1029/2022JC019249.

Howe, S., C. Miranda, C.T. Hayes, R.T. Letscher, and A.N. Knapp. 2020. The dual isotopic composition of nitrate in the Gulf of Mexico and Florida Straits. *Journal of Geophysical Research: Oceans* 125(9):e2020JC016047, https://doi.org/10.1029/2020JC016047.

Hutchings, L., C.D. van der Lingen, L.J. Shannon, R.J.M. Crawford, H.M.S. Verheye, C.H. Bartholomae, A.K. van der Plas, D. Louw, A. Kreiner, M. Ostrowski, and others. 2009. The Benguela Current: An ecosystem of four components. *Progress in Oceanography* 83(1):15–32, https://doi.org/10.1016/j.pocean.2009.07.046.

Izett, J.G., and K. Fennel. 2018. Estimating the cross-shelf export of riverine materials: Part 2. Estimates of global freshwater and nutrient export. *Global Biogeochemical Cycles* 32(2):176–186, https://doi.org/10.1002/2017GB005668.

Jayakumar, A., B.X. Chang, B. Widner, P. Bernhardt, M.R. Mulholland, and B.B. Ward. 2017. Biological nitrogen fixation in the oxygen-minimum region of the eastern tropical North Pacific Ocean. *The ISME Journal* 11(10):2,356–2,367, https://doi.org/10.1038/ismej.2017.97.

Jenkins, W.J., M. Hatta, J.N. Fitzsimmons, R. Schlitzer, N.T. Lanning, A. Shiller, N.R. Buckley, C.R. German, D.E. Lott, G. Weiss, and others. 2020. An intermediate-depth source of hydrothermal ^3He and dissolved iron in the North Pacific. *Earth and Planetary Science Letters* 539:116223, https://doi.org/10.1016/j.epsl.2020.116223.

Jickells, T.D., Z.S. An, K.K. Andersen, A.R. Baker, G. Bergametti, N. Brooks, J.J. Cao, P.W. Boyd, R.A. Duce, K.A. Hunter, and others. 2005. Global iron connections between desert dust, ocean biogeochemistry, and climate. *Science* 308(5718):67–71, https://doi.org/10.1126/science.1105959.

Jickells, T.D., E. Buitenhuis, K. Altieri, A.R. Baker, D. Capone, R.A. Duce, F. Dentener, K. Fennel, M. Kanakidou, J. LaRoche, and others. 2017. A reevaluation of the magnitude and impacts of anthropogenic atmospheric nitrogen inputs on the ocean. *Global Biogeochemical Cycles* 31(2):289–305, https://doi.org/10.1002/2016GB005586.

Karl, D., R. Letelier, L. Tupas, J. Dore, J. Christian, and D. Hebel. 1997. The role of nitrogen fixation in biogeochemical cycling in the subtropical North Pacific Ocean. *Nature*, 388(6642):533–538, https://doi.org/10.1038/41474.

Karsh, K.L., T.W. Trull, A.J. Lourey, and D.M. Sigman. 2003. Relationship of nitrogen isotope fractionation to phytoplankton size and iron availability during the Southern Ocean Iron RElease Experiment (SOIREE). *Limnology and Oceanography* 48(3):1,058–1,068, https://doi.org/10.4319/lo.2003.48.3.1058.

Karsh, K., J. Granger, K. Kritee, and D.M. Sigman. 2012. Eukaryotic assimilatory nitrate reductase fractionates N and O isotopes with a ratio near unity. *Environmental Science & Technology* 46:5,727–5,735, https://doi.org/10.1021/es204593q.

Kartal, B., and J.T. Keltjens. 2016. Anammox biochemistry: A tale of heme *c* proteins. *Trends in Biochemical Sciences* 41(12):998–1,011, https://doi.org/10.1016/j.tibs.2016.08.015.

Knapp, A.N., D.M. Sigman, and F. Lipschultz. 2005. N isotopic composition of dissolved organic nitrogen and nitrate at the Bermuda Atlantic Time-series Study site. *Global Biogeochemical Cycles* 19(1), https://doi.org/10.1029/2004GB002320.

Knapp, A.N., P.J. DiFiore, C. Deutsch, D.M. Sigman, and F. Lipschultz. 2008. Nitrate isotopic composition between Bermuda and Puerto Rico: Implications for N_2 fixation in the Atlantic Ocean. *Global Biogeochemical Cycles* 22(3), https://doi.org/10.1029/2007gb003107.

Knapp, A.N., D.M. Sigman, F. Lipschultz, A.B. Kustka, and D.G. Capone. 2011. Interbasin isotopic correspondence between upper-ocean bulk DON and subsurface nitrate and its implications for marine nitrogen cycling. *Global Biogeochemical Cycles* 25(4), https://doi.org/10.1029/2010GB003878.

Knapp, A., J. Dekaezemacker, S. Bonnet, J. Sohm, and D. Capone. 2012. Sensitivity of *Trichodesmium erythraeum* and *Crocosphaera watsonii* abundance and N_2 fixation rates to varying NO_3^- and PO_4^{3-} concentrations in batch cultures. *Aquatic Microbial Ecology* 66(3):223–236, https://doi.org/10.3354/ame01577.

Knapp, A.N., K.L. Casciotti, W.M. Berelson, M.G. Prokopenko, and D.G. Capone. 2016a. Low rates of nitrogen fixation in eastern tropical South Pacific surface waters. *Proceedings of the National Academy of Sciences of the United States of America* 113(16):4,398–4,403, https://doi.org/10.1073/pnas.1515641113.

Knapp, A.N., S.E. Fawcett, A. Martínez-Garcia, N. Leblond, T. Moutin, and S. Bonnet. 2016b. Nitrogen isotopic evidence for a shift from nitrate- to diazotroph-fueled export production in the VAHINE mesocosm experiments. *Biogeosciences* 13(16):4,645–4,657, https://doi.org/10.5194/bg-13-4645-2016.

Knapp, A.N., K.L. Casciotti, and M.G. Prokopenko. 2018. Dissolved organic nitrogen production and consumption in eastern tropical South Pacific surface waters. *Global Biogeochemical Cycles* 32(5):769–783, https://doi.org/10.1029/2017GB005875.

Knapp, A.N., R.K. Thomas, M.R. Stukel, T.B. Kelly, M.R. Landry, K.E. Selph, E. Malca, T. Gerard, and J. Lamkin. 2022. Constraining the sources of nitrogen fueling export production in the Gulf of Mexico using nitrogen isotope budgets. *Journal of Plankton Research* 44(5):692–710, https://doi.org/10.1093/plankt/fbab049.

Kritee, K., D.M. Sigman, J. Granger, B.B. Ward, A. Jayakumar, and C. Deutsch. 2012. Reduced isotope fractionation by denitrification under conditions relevant to the ocean. *Geochimica et Cosmochimica Acta* 92:243–259, https://doi.org/10.1016/j.gca.2012.05.020.

Kuypers, M.M.M., G. Lavik, D. Woebken, M. Schmid, B.M. Fuchs, R. Amann, B.B. Jorgensen, and M.S.M. Jetten. 2005. Massive nitrogen loss from the Benguela upwelling system through anaerobic ammonium oxidation. *Proceedings of the National Academy of Sciences of the United States of America* 102(18):6,478–6,483, https://doi.org/10.1073/pnas.0502088102.

Lam, P., G. Lavik, M.M. Jensen, J. van de Vossenberg, M. Schmid, D. Woebken, G. Dimitri, R. Amann, M.S.M. Jetten, and M.M.M. Kuypers. 2009. Revising the nitrogen cycle in the Peruvian oxygen minimum zone. *Proceedings of the National Academy of Sciences of the United States of America* 106(12):4,752–4,757, https://doi.org/10.1073/pnas.0812444106.

Landolfi, A., W. Koeve, H. Dietze, P. Kähler, and A. Oschlies. 2015. A new perspective on environmental controls of marine nitrogen fixation. *Geophysical Research Letters* 42(11):4,482–4,489, https://doi.org/10.1002/2015GL063756.

Landolfi, A., P. Kähler, W. Koeve, and A. Oschlies. 2018. Global marine N_2 fixation estimates: From observations to models. *Frontiers in Microbiology* 9:2112, https://doi.org/10.3389/fmicb.2018.02112.

Lehmann, M.F., D.M. Sigman, D.C. McCorkle, J. Granger, S. Hoffmann, G. Cane, and B.G. Brunelle. 2007. The distribution of nitrate $^{15}N/^{14}N$ in marine sediments and the impact of benthic nitrogen loss on the isotopic composition of oceanic nitrate. *Geochimica et Cosmochimica Acta* 71(22):5,384–5,404, https://doi.org/10.1016/j.gca.2007.07.025.

Lehmann, N., J. Granger, M. Kienast, K.S. Brown, P.A. Rafter, G. Martínez-Méndez, and M. Mohtadi. 2018. Isotopic evidence for the evolution of subsurface nitrate in the western equatorial Pacific. *Journal of Geophysical Research: Oceans* 123(3):1,684–1,707, https://doi.org/10.1002/2017JC013527.

Lehmann, N., M. Kienast, J. Granger, A. Bourbonnais, M.A. Altabet, and J. Tremblay. 2019. Remote western Arctic nutrients fuel remineralization in deep Baffin Bay. *Global Biogeochemical Cycles* 33(6):649–667, https://doi.org/10.1029/2018GB006134.

Letscher, R.T., D.A. Hansell, C.A. Carlson, R. Lumpkin, and A.N. Knapp. 2013. Dissolved organic nitrogen in the global surface ocean: Distribution and fate. *Global Biogeochemical Cycles* 27(1):141–153, https://doi.org/10.1029/2012GB004449.

Letscher, R.T., F. Primeau, and J.K. Moore. 2016. Nutrient budgets in the subtropical ocean gyres dominated by lateral transport. *Nature Geoscience* 9(11):815–821, https://doi.org/10.1038/ngeo2812.

Letscher, R.T., W.-L. Wang, Z. Liang, and A.N. Knapp. 2022. Regionally variable contribution of dissolved organic phosphorus to marine annual net community production. *Global Biogeochemical Cycles* 36(12):e2022GB007354, https://doi.org/10.1029/2022GB007354.

Liang, Z., R.T. Letscher, and A.N. Knapp. 2022a. Dissolved organic phosphorus concentrations in the surface ocean controlled by both phosphate and iron stress. *Nature Geoscience* 15(8):651–657, https://doi.org/10.1038/s41561-022-00988-1.

Liang, Z., K. McCabe, S.E. Fawcett, H.J. Forrer, F. Hashihama, C. Jeandel, D. Marconi, H. Planquette, M.A. Saito, J.A. Sohm, and others. 2022b. A global ocean dissolved organic phosphorus concentration database (DOPv2021). *Scientific Data* 9(1):772, https://doi.org/10.1038/s41597-022-01873-7.

Liang, Z., R.T. Letscher, and A.N. Knapp. 2023. Global patterns of surface ocean dissolved organic matter stoichiometry. *Global Biogeochemical Cycles* 37:e2023GB007788, https://doi.org/10.1029/2023GB007788.

Lourey, M.J., T.W. Trull, and D.M. Sigman. 2003. Sensitivity of $\delta^{15}N$ of nitrate, surface suspended and deep sinking particulate nitrogen to seasonal nitrate depletion in the Southern Ocean. *Global Biogeochemical Cycles* 17(3), https://doi.org/10.1029/2002GB001973.

Luo, Y.-W., S.C. Doney, L.A. Anderson, M. Benavides, I. Berman-Frank, A. Bode, S. Bonnet, K.H. Boström, D. Böttjer, D.G. Capone, and others. 2012. Database of diazotrophs in global ocean: Abundance, biomass and nitrogen fixation rates. *Earth System Science Data* 4(1):47–73, https://doi.org/10.5194/essd-4-47-2012.

Mahowald, N.M., A.R. Baker, G. Bergametti, N. Brooks, R.A. Duce, T.D. Jickells, N. Kubilay, J.M. Prospero, and I. Tegen. 2005. Atmospheric global dust cycle and iron inputs to the ocean. *Global Biogeochemical Cycles* 19(4), https://doi.org/10.1029/2004GB002402.

Mahowald, N.M., S. Engelstaedter, C. Luo, A. Sealy, P. Artaxo, C. Benitez-Nelson, S. Bonnet, Y. Chen, P.Y. Chuang, D.D. Cohen, and others. 2009. Atmospheric iron deposition: Global distribution, variability, and human perturbations. *Annual Review of Marine Science* 1:245–278, https://doi.org/10.1146/annurev.marine.010908.163727.

Marconi, D., M. Alexandra Weigand, P.A. Rafter, M.R. McIlvin, M. Forbes, K.L. Casciotti, and D.M. Sigman. 2015. Nitrate isotope distributions on the US GEOTRACES North Atlantic cross-basin section: Signals of polar nitrate sources and low latitude nitrogen cycling. *Marine Chemistry* 177:143–156, https://doi.org/10.1016/j.marchem.2015.06.007.

Marconi, D., S. Kopf, P.A. Rafter, and D.M. Sigman. 2017a. Aerobic respiration along isopycnals leads to overestimation of the isotope effect of denitrification in the ocean water column. *Geochimica et Cosmochimica Acta* 197:417–432, https://doi.org/10.1016/j.gca.2016.10.012.

Marconi, D., D M. Sigman, K.L. Casciotti, E.C. Campbell, M.A. Weigand, S.E. Fawcett, A.N. Knapp, P.A. Rafter, B.B. Ward, and G.H. Haug. 2017b. Tropical dominance of N_2 fixation in the North Atlantic Ocean. *Global Biogeochemical Cycles* 31(10), https://doi.org/10.1002/2016GB005613.

Marconi, D., M.A. Weigand, and D.M. Sigman. 2019. Nitrate isotopic gradients in the North Atlantic Ocean and the nitrogen isotopic composition of sinking organic matter. *Deep Sea Research Part I* 145:109–124, https://doi.org/10.1016/j.dsr.2019.01.010.

Mariotti, A., J.C. Germon, P. Hubert, P. Kaiser, R. Letolle, A. Tardieux, and P. Tardieux. 1981. Experimental determination of nitrogen kinetic isotope fractionation: Dome principles; Illustration for the denitrification and nitrification processes. *Plant and Soil* 62:413–430, https://doi.org/10.1007/BF02374138.

Marshall, T., J. Granger, K.L. Casciotti, K. Dähnke, K.C. Emeis, D. Marconi, M.R. McIlvin, A.E. Noble, M.A. Saito, D.M. Sigman, and S.E. Fawcett. 2022. The Angola Gyre is a hotspot of dinitrogen fixation in the South Atlantic Ocean. *Communications Earth and Environment* 3:151, https://doi.org/10.1038/s43247-022-00474-x.

Marshall, T.A., D.M. Sigman, L.M. Beal, A. Foreman, A. Martínez-García, S. Blain, E. Campbell, F. Fripiat, R. Granger, E. Harris, and others. 2023. The Agulhas Current transports signals of local and remote Indian Ocean nitrogen cycling. *Journal of Geophysical Research: Oceans* 128(3):e2022JC019413, https://doi.org/10.1029/2022JC019413.

Martin, J.H., M. Gordon, and S.E. Fitzwater. 1991. The case for iron. *Limnology and Oceanography* 36(8):1,793–1,802, https://doi.org/10.4319/lo.1991.36.8.1793.

Martin, T.S., F. Primeau, and K.L. Casciotti. 2019a. Assessing marine nitrogen cycle rates and process sensitivities with a global 3-D inverse model. *Global Biogeochemical Cycles* 33(8), https://doi.org/10.1029/2018GB006088.

Martin, T.S., F. Primeau, and K.L. Casciotti. 2019b. Modeling oceanic nitrate and nitrite concentrations and isotopes using a 3-D inverse N cycle model. *Biogeosciences*, https://doi.org/10.5194/bg-16-347-2019.

Martiny, A.C., C.T.A. Pham, F.W. Primeau, J.A. Vrugt, J.K. Moore, S.A. Levin, and M.W. Lomas. 2013. Strong latitudinal patterns in the elemental ratios of marine plankton and organic matter. *Nature Geoscience* 6(4):279–283, https://doi.org/10.1038/ngeo1757.

Matiatos, I., L.I. Wassenaar, L.R. Monteiro, J.J. Venkiteswaran, D.C. Gooddy, P. Boeckx, E. Sacchi, F.-J. Yue, G. Michalski,

C. Alonso-Hernández, and others. 2021. Global patterns of nitrate isotope composition in rivers and adjacent aquifers reveal reactive nitrogen cascading. *Communications Earth & Environment* 2:52, https://doi.org/10.1038/s43247-021-00121-x.

Mellett, T., and K.N. Buck. 2020. Spatial and temporal variability of trace metals (Fe, Cu, Mn, Zn, Co, Ni, Cd, Pb), iron and copper speciation, and electroactive Fe-binding humic substances in surface waters of the eastern Gulf of Mexico. *Marine Chemistry* 227:103891, https://doi.org/10.1016/j.marchem.2020.103891.

Mills, M.M., C. Ridame, M. Davey, J. La Roche, and R.J. Geider. 2004. Iron and phosphorus co-limit nitrogen fixation in the eastern tropical North Atlantic. *Nature* 429(6989):292–294, https://doi.org/10.1038/nature02550.

Mills, M.M., and K.R. Arrigo. 2010. Magnitude of oceanic nitrogen fixation influenced by the nutrient uptake ratio of phytoplankton. *Nature Geoscience* 3(6):412–416, https://doi.org/10.1038/ngeo856.

Montoya, J.P., M. Voss, P. Kahler, and D.G. Capone. 1996. A simple, high-precision, high-sensitivity tracer assay for N(inf2) fixation. *Applied and Environmental Microbiology* 62(3):986–993, https://doi.org/10.1128/aem.62.3.986-993.1996.

Montoya, J.P., E. Carpenter, and D. Capone. 2002. Nitrogen fixation and nitrogen isotope abundance in zooplankton of the oligotrophic North Atlantic. *Limnology and Oceanography* 47:1,617–1,628, https://doi.org/10.4319/lo.2002.47.6.1617.

Moore, C.M., M.M. Mills, E.P. Achterberg, R.J. Geider, J. LaRoche, M.I. Lucas, E.L. McDonagh, X. Pan, A.J. Poulton, M.J.A. Rijkenberg, and others. 2009. Large-scale distribution of Atlantic nitrogen fixation controlled by iron availability. *Nature Geoscience* 2(12):867–871, https://doi.org/10.1038/ngeo667.

Morel, F.M.M., and N.M. Price. 2003. The biogeochemical cycles of trace metals in the oceans. *Science* 300(5621):944–947, https://doi.org/10.1126/science.1083545.

Morel, F.M.M., P.J. Lam, and M.A. Saito. 2020. Trace metal substitution in marine phytoplankton. *Annual Review of Earth and Planetary Sciences* 48(1):491–517, https://doi.org/10.1146/annurev-earth-053018-060108.

Noble, A.E., C.H. Lamborg, D.C. Ohnemus, P.J. Lam, T.J. Goepfert, C.I. Measures, C.H. Frame, K.L. Casciotti, G.R. DiTullio, J. Jennings, and M.A. Saito. 2012. Basin-scale inputs of cobalt, iron, and manganese from the Benguela-Angola front to the South Atlantic Ocean. *Limnology and Oceanography* 57(4):989–1,010, https://doi.org/10.4319/lo.2012.57.4.0989.

Orchard, E.D., J.W. Ammerman, M.W. Lomas, and S.T. Dyhrman. 2010. Dissolved inorganic and organic phosphorus uptake in *Trichodesmium* and the microbial community: The importance of phosphorus ester in the Sargasso Sea. *Limnology and Oceanography* 55(3):1,390–1,399, https://doi.org/10.4319/lo.2010.55.3.1390.

Palenik, B., and F.M.M. Morel. 1991. Amine oxidases of marine phytoplankton. *Applied and Environmental Microbiology* 57(8):2,440–2,443, https://doi.org/10.1128/aem.57.8.2440-2443.1991.

Peters, B., R. Horak, A. Devol, C. Fuchsman, M. Forbes, C.W. Mordy, and K.L. Casciotti. 2018a. Estimating fixed nitrogen loss and associated isotope effects using concentration and isotope measurements of NO_3^-, NO_2^-, and N_2 from the eastern tropical South Pacific oxygen deficient zone. *Deep Sea Research Part II* 156:121–136, https://doi.org/10.1016/j.dsr2.2018.02.011.

Peters, B.D., P.J. Lam, and K.L. Casciotti. 2018b. Nitrogen and oxygen isotope measurements of nitrate along the US GEOTRACES Eastern Pacific Zonal Transect (GP16) yield insights into nitrate supply, remineralization, and water mass transport. *Marine Chemistry* 201:137–150, https://doi.org/10.1016/j.marchem.2017.09.009.

Rabalais, N.N., R.E. Turner, D. Justić, Q. Dortch, W.J. Wiseman, and B.K. Sen Gupta. 1996. Nutrient changes in the Mississippi River and system responses on the adjacent continental shelf. *Estuaries* 19(2):386–407, https://doi.org/10.2307/1352458.

Rafter, P.A., D.M. Sigman, C.D. Charles, J. Kaiser, and G.H. Haug. 2012. Subsurface tropical Pacific nitrogen isotopic composition of nitrate: Biogeochemical signals and their transport. *Global Biogeochemical Cycles* 26(1), https://doi.org/10.1029/2010GB003979.

Rafter, P.A., P.J. DiFiore, and D.M. Sigman. 2013. Coupled nitrate nitrogen and oxygen isotopes and organic matter remineralization in the Southern and Pacific Oceans. *Journal of Geophysical Research: Oceans* 118(10):4,781–4,794, https://doi.org/10.1002/jgrc.20316.

Rafter, P.A., D.M. Sigman, and K.R.M. Mackey. 2017. Recycled iron fuels new production in the eastern equatorial Pacific Ocean. *Nature Communications* 8(1):1100, https://doi.org/10.1038/s41467-017-01219-7.

Rafter, P.A., A. Bagnell, D. Marconi, and T. DeVries. 2019. Global trends in marine nitrate N isotopes from observations and a neural network-based climatology. *Biogeosciences* 16(13):2,617–2,633, https://doi.org/10.5194/bg-16-2617-2019.

Rafter, P.A. 2024. On the variability of equatorial Pacific nitrate and iron utilization. *Oceanography* 37(2), https://doi.org/10.5670/oceanog.2024.411.

Redfield, A.C., B.H. Ketchum, and F.A. Richards. 1963. The influence of organisms on the composition of seawater. Pp. 26–77 in *The Sea*, vol. 2. M.N. Hill, ed., Interscience, New York.

Resing, J.A., P.N. Sedwick, C.R. German, W.J. Jenkins, J.W. Moffett, B.M. Sohst, and A. Tagliabue. 2015. Basin-scale transport of hydrothermal dissolved metals across the South Pacific Ocean. *Nature* 523(7559):200–203, https://doi.org/10.1038/nature14577.

Rijkenberg, M.J.A., R. Middag, P. Laan, L.J.A. Gerringa, H.M. van Aken, V. Schoemann, J.T.M. de Jong, and H.J.W. de Baar. 2014. The distribution of dissolved iron in the West Atlantic Ocean. *PLoS ONE* 9(6):e101323, https://doi.org/10.1371/journal.pone.0101323.

Rohde, M.M., J. Granger, D.M. Sigman, and M.F. Lehmann. 2015. Coupled nitrate N and O stable isotope fractionation by a natural marine plankton consortium. *Frontiers in Marine Science* 2:28, https://doi.org/10.3389/fmars.2015.00028.

Romera-Castillo, C., R.T. Letscher, and D.A. Hansell. 2016. New nutrients exert fundamental control on dissolved organic carbon accumulation in the surface Atlantic Ocean. *Proceedings of the National Academy of Sciences of the United States of America* 113(38):10,497–10,502, https://doi.org/10.1073/pnas.1605344113.

Saito, M.A., M.R. McIlvin, D.M. Moran, A.E. Santoro, C.L. Dupont, P.A. Rafter, J.K. Saunders, D. Kaul, C.H. Lamborg, M. Westley, and others. 2020. Abundant nitrite-oxidizing metalloenzymes in the mesopelagic zone of the tropical Pacific Ocean. *Nature Geoscience* 13(5):355–362, https://doi.org/10.1038/s41561-020-0565-6.

Santos, I.R., X. Chen, A.L. Lecher, A.H. Sawyer, N. Moosdorf, V. Rodellas, J. Tamborski, H.-M. Cho, N. Dimova, R. Sugimoto, and others. 2021. Submarine groundwater discharge impacts on coastal nutrient biogeochemistry. *Nature Reviews Earth & Environment* 2(5):307–323, https://doi.org/10.1038/s43017-021-00152-0.

Seitzinger, S.P., E. Mayorga, A.F. Bouwman, C. Kroeze, A.H.W. Beusen, G. Billen, G. Van Drecht, E. Dumont, B M. Fekete, J. Garnier, and J.A. Harrison. 2010. Global river nutrient export: A scenario analysis of past and future trends. *Global Biogeochemical Cycles* 24(4), https://doi.org/10.1029/2009GB003587.

Shafiee, R.T., J.T. Snow, Q. Zhang, and R.E.M. Rickaby. 2019. Iron requirements and uptake strategies of the globally abundant marine ammonia-oxidising archaeon, *Nitrosopumilus maritimus* SCM1. *The ISME Journal* 13(9):2,295–2,305, https://doi.org/10.1038/s41396-019-0434-8.

Shao, Z., Y. Xu, H. Wang, W. Luo, L. Wang, Y. Huang, N.S.R. Agawin, A. Ahmed, M. Benavides, M. Bentzon-Tilia, and others. 2023. Global oceanic diazotroph database version 2 and elevated estimate of global oceanic N_2 fixation. *Earth System Science Data* 15(8):3,673–3,709, https://doi.org/10.5194/essd-15-3673-2023.

Sharples, J., J.J. Middelburg, K. Fennel, and T.D. Jickells. 2017. What proportion of riverine nutrients reaches the open ocean? *Global Biogeochemical Cycles* 31(1):39–58, https://doi.org/10.1002/2016GB005483.

Sigman, D.M., M.A. Altabet, R. François, D.C. McCorkle, and G. Fischer. 1999. The $\delta^{15}N$ of nitrate in the Southern Ocean: Consumption of nitrate in surface waters. *Global Biogeochemical Cycles* 13(4):1,149–1,166, https://doi.org/10.1029/1999GB900038.

Sigman, D.M., M.A. Altabet, D.C. McCorkle, R. François, and G. Fischer. 2000. The $\delta^{15}N$ of nitrate in the Southern Ocean: Nitrogen cycling and circulation in the ocean interior. *Journal of Geophysical Research: Oceans* 105(C8):19,599–19,614, https://doi.org/10.1029/2000JC000265.

Sigman, D.M., J. Granger, P.J. DiFiore, M.M.F. Lehmann, R. Ho, G. Cane, and A. van Geen. 2005. Coupled nitrogen and oxygen isotope measurements of nitrate along the eastern North Pacific margin. *Global Biogeochemical Cycles* 19(4), https://doi.org/10.1029/2005GB002458.

Sigman, D.M., P.J. DiFiore, M.P. Hain, C. Deutsch, Y. Wang, D.M. Karl, A.N. Knapp, M.F. Lehman, S. Pantoja, and M.F. Lehmann. 2009. The dual isotopes of deep nitrate as a constraint on the cycle and budget of oceanic fixed nitrogen. *Deep Sea Research Part I* 56(9):1,419–1,439, https://doi.org/10.1016/j.dsr.2009.04.007.

Sigman, D.M., M.P. Hain, and G.H. Haug. 2010. The polar ocean and glacial cycles in atmospheric CO_2 concentration. *Nature* 466(7302):47–55, https://doi.org/10.1038/nature09149.

Sigman, D.M., and F. Fripiat. 2019. Nitrogen isotopes in the ocean. Pp. 263–278 in *Encyclopedia of Ocean Sciences*. J.K. Cochran, H.J. Bokuniewicz, and P.L. Yager, eds, Elsevier, https://doi.org/10.1016/B978-0-12-409548-9.11605-7.

Smart, S.M., S.E. Fawcett, S.J. Thomalla, M.A. Weigand, C.J.C. Reason, and D.M. Sigman. 2015. Isotopic evidence for nitrification in the Antarctic winter mixed layer. *Global Biogeochemical Cycles* 29(4):427–445, https://doi.org/10.1002/2014GB005013.

Snow, J.T., D. Polyviou, P. Skipp, N.A.M. Chrismas, A. Hitchcock, R. Geider, C.M. Moore, and T.S. Bibby. 2015. Quantifying integrated proteomic responses to iron stress in the globally important marine diazotroph *Trichodesmium*. *PLoS ONE* 10(11):e0142626, https://doi.org/10.1371/journal.pone.0142626.

Sohm, J., and D. Capone. 2006. Phosphorus dynamics of the tropical and subtropical North Atlantic: *Trichodesmium* spp. versus bulk plankton. *Marine Ecology Progress Series* 317:21–28, https://doi.org/10.3354/meps317021.

Sohm, J.A., J.A. Hilton, A.E. Noble, J.P. Zehr, M.A. Saito, and E.A. Webb. 2011. Nitrogen fixation in the South Atlantic Gyre and the Benguela Upwelling System. *Geophysical Research Letters* 38(16), https://doi.org/10.1029/2011GL048315.

Somes, C.J., A. Schmittner, E.D. Galbraith, M.F. Lehmann, M.A. Altabet, J.P. Montoya, R.M. Letelier, A.C. Mix, A. Bourbonnais, and M. Eby. 2010. Simulating the global distribution of nitrogen isotopes in the ocean. *Global Biogeochemical Cycles* 24(4), https://doi.org/10.1029/2009gb003767.

Somes, C.J., A. Oschlies, and A. Schmittner. 2013. Isotopic constraints on the pre-industrial oceanic nitrogen budget. *Biogeosciences* 10(9):5,889–5,910, https://doi.org/10.5194/bg-10-5889-2013.

Stein, L.Y. 2019. Insights into the physiology of ammonia-oxidizing microorganisms. *Current Opinion in Chemical Biology* 49:9–15, https://doi.org/10.1016/j.cbpa.2018.09.003.

Subramaniam, A., P.L. Yager, E.J. Carpenter, C. Mahaffey, K. Björkman, S. Cooley, A.B. Kustka, J.P. Montoya, S.A. Sañudo-Wilhelmy, R. Shipe, and D.G. Capone. 2008. Amazon River enhances diazotrophy and carbon sequestration in the tropical North Atlantic Ocean. *Proceedings of the National Academy of Sciences of the United States of America* 105(30):10,460–10,465, https://doi.org/10.1073/pnas.0710279105.

Sun, X., C. Frey, and B.B. Ward. 2023. Nitrite oxidation across the full oxygen spectrum in the ocean. *Global Biogeochemical Cycles* 37(4):e2022GB007548, https://doi.org/10.1029/2022GB007548.

Tagliabue, A., L. Bopp, J.-C. Dutay, A.R. Bowie, F. Chever, P. Jean-Baptiste, E. Bucciarelli, D. Lannuzel, T. Remenyi, G. Sarthou, and others. 2010. Hydrothermal contribution to the oceanic dissolved iron inventory. *Nature Geoscience* 3(4):252–256, https://doi.org/10.1038/ngeo818.

Tagliabue, A., A.R. Bowie, T. DeVries, M.J. Ellwood, W.M. Landing, A. Milne, D.C. Ohnemus, B.S. Twining, and P.W. Boyd. 2019. The interplay between regeneration and scavenging fluxes drives ocean iron cycling. *Nature Communications* 10(1):4960, https://doi.org/10.1038/s41467-019-12775-5.

Tagliabue, A., A.R. Bowie, T. Holmes, P. Latour, P. van der Merwe, M. Gault-Ringold, K. Wuttig, and J.A. Resing. 2022. Constraining the contribution of hydrothermal iron to Southern Ocean export production using deep ocean iron observations. *Frontiers in Marine Science* 9:754517, https://doi.org/10.3389/fmars.2022.754517.

Torres-Valdes, S., V.M. Roussenov, R. Sanders, S. Reynolds, X. Pan, R. Mather, A. Landolfi, G.A. Wolff, E.P. Achterberg, and R.G. Williams. 2009. Distribution of dissolved organic nutrients and their effect on export production over the Atlantic Ocean. *Global Biogeochemical Cycles* 23(4), https://doi.org/10.1029/2008gb003389.

Tuerena, R.E., R.S. Ganeshram, W. Geibert, A.E. Fallick, J. Dougans, A. Tait, S.F. Henley, and E.M.S. Woodward. 2015. Nutrient cycling in the Atlantic basin: The evolution of nitrate isotope signatures in water masses. *Global Biogeochemical Cycles* 29(10):1,830–1,844, https://doi.org/10.1002/2015GB005164.

Turk-Kubo, K.A., M. Karamchandani, D.G. Capone, and J.P. Zehr. 2014. The paradox of marine heterotrophic nitrogen fixation: Abundances of heterotrophic diazotrophs do not account for nitrogen fixation rates in the eastern tropical South Pacific. *Environmental Microbiology* 16(10):3,095–3,114, https://doi.org/10.1111/1462-2920.12346.

Vieira, L.H., S. Krisch, M.J. Hopwood, A.J. Beck, J. Scholten, V. Liebetrau, and E.P. Achterberg. 2020. Unprecedented Fe delivery from the Congo River margin to the South Atlantic Gyre. *Nature Communications* 11(1):556, https://doi.org/10.1038/s41467-019-14255-2.

Voss, M., J.W. Dippner, and J.P. Montoya. 2001. Nitrogen isotope patterns in the oxygen-deficient waters of the Eastern Tropical North Pacific Ocean. *Deep Sea Research Part I* 48(8):1,905–1,921, https://doi.org/10.1016/S0967-0637(00)00110-2.

Wan, X.S., L. Hou, S.-J. Kao, Y. Zhang, H.-X. Sheng, H. Shen, S. Tong, W. Qin, and B.B. Ward. 2023. Pathways of N_2O production by marine ammonia-oxidizing archaea determined from dual-isotope labeling. *Proceedings of the National Academy of Sciences of the United States of America* 120(11):e2220697120, https://doi.org/10.1073/pnas.2220697120.

Wang, W.L., J.K. Moore, A.C. Martiny, and F.W. Primeau. 2019. Convergent estimates of marine nitrogen fixation. *Nature* 566:205–211, https://doi.org/10.1038/s41586-019-0911-2.

Wankel, S.D., C. Kendall, J.T. Pennington, F.P. Chavez, and A. Paytan. 2007. Nitrification in the euphotic zone as evidenced by nitrate dual isotopic composition: Observations from Monterey Bay, California. *Global Biogeochemical Cycles* 21(2), https://doi.org/10.1029/2006GB002723.

Ward, B.B. 2013. Oceans. How nitrogen is lost. *Science* 341(6144):352–353, https://doi.org/10.1126/science.1240314.

Weber, T., and C. Deutsch. 2014. Local versus basin-scale limitation of marine nitrogen fixation. *Proceedings of the National Academy of Sciences of the United States of America* 111(24):8,741–8,746, https://doi.org/10.1073/pnas.1317193111.

Wei, X., N. Vajrala, L. Hauser, L.A. Sayavedra-Soto, and D.J. Arp. 2006. Iron nutrition and physiological responses to iron stress in *Nitrosomonas europaea*. *Archives of Microbiology* 186(2):107–118, https://doi.org/10.1007/s00203-006-0126-4.

Wen, Z., T.J. Browning, Y. Cai, R. Dai, R. Zhang, C. Du, R. Jiang, W. Lin, X. Liu, Z. Cao, and others. 2022. Nutrient regulation of biological nitrogen fixation across the tropical western North Pacific. *Science Advances* 8(5):eabl7564, https://doi.org/10.1126/sciadv.abl7564.

White, A.E., Y.H. Spitz, D.M. Karl, and R.M. Letelier. 2006. Flexible elemental stoichiometry in *Trichodesmium* spp. and its ecological implications. *Limnology and Oceanography* 51(4):1,777–1,790, https://doi.org/10.4319/lo.2006.51.4.1777.

White, A.E., J. Granger, C. Selden, M.R. Gradoville, L. Potts, A. Bourbonnais, R.W. Fulweiler, A.N. Knapp, W. Mohr, P.H. Moisander, and others. 2020. A critical review of the $^{15}N_2$ tracer method to measure diazotrophic production in pelagic ecosystems. *Limnology and Oceanography: Methods* 18(4):129–147, https://doi.org/10.1002/lom3.10353.

Yang, S., and N. Gruber. 2016. The anthropogenic perturbation of the marine nitrogen cycle by atmospheric deposition: Nitrogen cycle feedbacks and the ^{15}N Haber-Bosch effect. *Global Biogeochemical Cycles* 30(10):1,418–1,440, https://doi.org/10.1002/2016GB005421.

Yoshikawa, C., A. Makabe, T. Shiozaki, S. Toyoda, O. Yoshida, K. Furuya, and N. Yoshida. 2015. Nitrogen isotope ratios of nitrate and N* anomalies in the subtropical South Pacific. *Geochemistry, Geophysics, Geosystems* 16(5):1,439–1,448, https://doi.org/10.1002/2014GC005678.

Zehr, J.P., and D.G. Capone. 2020. Changing perspectives in marine nitrogen fixation. *Science* 368(6492), https://doi.org/10.1126/science.aay9514.

Zhang, R., X.T. Wang, H. Ren, J. Huang, M. Chen, and D.M. Sigman. 2020. Dissolved organic nitrogen cycling in the South China Sea from an isotopic perspective. *Global Biogeochemical Cycles* 34(12):e2020GB006551, https://doi.org/10.1029/2020GB006551.

Zumft, W.G. 1997. Cell biology and molecular basis of denitrification. *Microbiology and Molecular Biology Reviews* 61(4):533–616, https://doi.org/10.1128/mmbr.61.4.533-616.1997.

ACKNOWLEDGMENTS

The authors would like to gratefully acknowledge the international efforts and cooperation involved with the collection of the data and interpretations that formed the basis for this review. The International GEOTRACES Program is possible in part thanks to support from the US National Science Foundation (NSF) grant OCE-2140395 to the Scientific Committee on Oceanic Research (SCOR). The authors would like to thank guest editors Tim Conway, Jessica Fitzsimmons, Hélène Planquette, Taryn Noble, and Rob Middag for their handling of this manuscript, as well as Patrick Rafter and an anonymous reviewer for their insightful comments on an earlier draft. We are also thankful to Reiner Schlitzer for graciously producing the graphics used in Figure 3. KLC acknowledges support from NSF award OCE-2048961. ANK acknowledges support from NSF OCE-2148989. SF thanks the South African National Research Foundation (116142, 150540, and SANAP230527110611) and the University of Cape Town Vice-Chancellor's Future Leaders 2030 program. TM and SF acknowledge the South African Department of Science and Innovation's Biogeochemistry Research Infrastructure Platform (BIOGRIP).

AUTHORS

Karen L. Casciotti (kcasciotti@stanford.edu) is Professor, Oceans Department, Stanford University, Stanford, CA, USA. **Tanya A. Marshall** is Postdoctoral Researcher, Department of Oceanography, University of Cape Town, Cape Town, South Africa. **Sarah E. Fawcett** is Associate Professor, Department of Oceanography, University of Cape Town, Cape Town, South Africa. **Angela N. Knapp** is Associate Professor, Earth, Ocean, and Atmospheric Science Department, Florida State University, Tallahassee, FL, USA.

ARTICLE CITATION

Casciotti, K.L., T.A. Marshall, S.E. Fawcett, and A.N. Knapp. 2024. Advances in understanding the marine nitrogen cycle in the GEOTRACES era. *Oceanography* 37(2), https://doi.org/10.5670/oceanog.2024.406.

COPYRIGHT & USAGE